Separation of poly(acrylic acid) salts according to topology using capillary electrophoresis in the critical conditions

Alison R Maniego, Dale Ang, Yohann Guillaneuf, Catherine Lefay, Didier Gigmes, Janice R Aldrich-Wright, Marianne Gaborieau, Patrice Castignolles

Alison R. Maniego,[1,2] Dale Ang,[1,2] Yohann Guillaneuf*,[3] Catherine Lefay,[3] Didier Gigmes,[3]

Janice R. Aldrich-Wright,[2] Marianne Gaborieau,[2] Patrice Castignolles[1,*]

Separation of poly(acrylic acid) salts according to the topology using capillary electrophoresis in the critical conditions

[1] University of Western Sydney (UWS), Australian Centre for Research on Separation Sciences (ACROSS), School of Science and Health, Parramatta campus, Locked Bag 1797, Penrith NSW 2751, Australia

[2] University of Western Sydney (UWS), School of Science and Health, Nanoscale Organisation and Dynamics group, Locked Bag 1797, Penrith NSW 2751, Australia

[3] Aix-Marseille Université, CNRS, Institut de Chimie Radicalaire, UMR 7273, 13397, Marseille, France

* Corresponding author: p.castignolles@uws.edu.au, phone +61 2 9685 9970, fax +61 2 9685 9915

Abstract:

Branching was detected in polyacrylates synthesised through radical polymerization via solution-state NMR, while inconsistencies had been reported for the determination of the molar mass of hydrophilic polyacrylates between aqueous-phase and organic-phase size-exclusion chromatography (SEC). In this work, poly(sodium acrylate)s, PNaAs, of various topologies were separated for the first time using free-solution capillary electrophoresis. Free-solution CE does not separate the PNaAs by their molar mass, similarly to separations by liquid chromatography in the critical conditions. PNaAs with different topologies (linear, star branched and hyperbranched) were separated using free-solution CE. The electrophoretic mobility of PNaAs increases as the degree of branching decreases. Separation is shown to be not only by the topology but also by the end groups as expected for a separation in the critical conditions: replacing a relatively bulky nitroxide end group with hydrogen atom yielded a higher electrophoretic mobility. This novel method, capillary electrophoresis in the critical conditions enabled, for the first time, the characterization of hydrophilic polyacrylates according to their topology (branching) and their chain ends. This will enable meaningful and accurate characterization of their branched topologies as well as molar masses and enable advances for advanced applications such as drug delivery or flocculation.

Keywords Poly(acrylic acid); Branching; Topology; Capillary Electrophoresis; Chain End analysis;

Introduction

Water-soluble polyacrylates represent an important type of industrial polymer which is found in many applications ranging from commodity use to high value materials.[1] In particular, the primary uses include disposable hygiene applications such as baby diapers, and feminine hygiene products. Other industrial/technical applications are typically more long-life applications, including protective coatings for electrical cable, food packaging, medical/medical waste adsorbents, agricultural/horticultural soil adsorbents, lubricants/sealants, cosmetics, and stabilizing agents/thickeners in coatings. Poly(acrylic acid) and its salts are the focus of intensive research for advanced applications for example as additives for controlled mineralization [2, 3], nano-reactors and drug carrier systems [4].

Polyacrylics produced by radical polymerization undergo both intra and intermolecular H-transfer leading to branched polymer chains,[5, 6] including when produced by controlled polymerization, such as nitroxide-mediated polymerization [7, 8]. This phenomenon is now qualitatively understood for polyacrylates, and some kinetic rate constants for intramolecular and intermolecular H-transfer have already been determined for poly(alkyl acrylate)s. The branching in water-soluble polyacrylates received less attention but the occurrence of transfer to polymer in the radical polymerization of acrylic acid has been demonstrated.[9-11] The aim of this work is to characterize branching in poly(acrylic acid) (PAA). Branching can also be introduced in the PAA through multifunctional initiators and inimers.[12, 13] ^{13}C nuclear magnetic resonance spectroscopy (NMR) can be used to detect and quantify the branching resulting from inter- and intramolecular transfer to polymer in poly(alkyl acrylate)s [14-16] as well as poly(acrylic acid)[10, 11]. This is done through the detection of the quaternary carbon at the branching point. The samples synthesized in this work with house-made initiators have additional branching points of a different chemical nature from this quaternary carbon, which have never been investigated through NMR. ^{13}C NMR yields an average degree of branching, which corresponds to an average number of branches relative to the total number of monomer units.[14] NMR yields no information on the distribution of branching structures inside the sample, for which a separation method is needed. NMR may also have a limited sensitivity to low levels of long branches which may significantly affect the separation with CE-CC.

Aqueous size-exclusion chromatography (SEC) is currently the most widely used technique for the analysis of hydrophilic polyacrylates. However, it is controversial since aqueous SEC of polyacrylates and SEC of the same methylated polyacrylates in tetrahydrofuran yield significantly different molar masses.[17] Furthermore, separation of statistically branched polymers can lead to incomplete SEC separation in terms of molar mass.[18] In the case of hydrophobic polyacrylates, errors up to 100 % were measured for determined molar masses using multiple detection SEC and the concept of local dispersity.[19, 20] Other forms of liquid chromatography are increasingly used for polymers with complex architectures and use critical conditions, i.e. conditions where one component is not separated according to its molar mass. The most popular is liquid chromatography at the point of exclusion-adsorption transition, also called liquid chromatography in the critical conditions, LC-CC.[21-23] LC-CC is complementary to SEC [24-26] but its robustness is usually limited in terms of molar mass range, recovery,[27] influence of the history of the column [28] and this method requires tedious optimization [29]. Separation of charged or generally hydrophilic polymers presents additional challenges in order to use HPLC.[30] The composition of copolymers of poly(acrylic acid) salts has been investigated once using liquid

chromatography in the critical conditions,[31] but not their branching. The separation of PAA chains according to their topology will be worthwhile since this property critically affects its efficiency for many applications. This had never been published to the best of our knowledge.

Capillary electrophoresis is widely applied to a few biopolymers, DNA and proteins, but not to other biopolymers or synthetic polymers. Capillary gel electrophoresis has been explored for polymer separations leading to a similar type of separation than SEC,[32] but facing a number of its limitations as well such as the varying accuracy of apparent molar masses,[33] the influence of branching on a separation by size and not be molar mass, etc. Free-solution capillary electrophoresis has been little applied to polymer separations but with success.[34, 35] Hoagland *et al.* performed free-solution capillary electrophoresis of poly(sodium acrylate) (PNaA) and some copolymers to study their charge.[36] Cottet *et al.* then showed that PNaAs, as other tested polyelectrolytes, are not separated by molar mass when the number of monomer units is well above 10,[37] corresponding to the critical conditions sought in liquid chromatography (although the mechanism of separation is different, the mode is the same). We confirmed this by studying the separation of different salts of oligo(acrylic acid). The resolution of free-solution CE was found superior to the one of SEC.[38] Coupling with electrospray ionization – time of flight mass spectrometry (ESI TOF MS) showed that free-solution CE separates oligoacrylates according to the number of monomer units, but also according to the stereochemistry (tacticity).[39] It also confirmed that free-solution CE is CE in the critical conditions (CE-CC) for poly(acrylic acid) salts, as there is no separation of the homopolymer according to its molar mass. This mode of separation has also been observed in the case of poly(styrene sulfonate)[40] as well as DNA[41]. CE-CC was validated in terms of repeatability through the characterization of gellan gums.[42] Furthermore the method displayed a fast separation of gellan gums in terms of the differences in their composition. Dendrimers of different generations exhibit different electrophoretic mobilities [43] and separation by branching is thus expected in CE-CC, with no influence of the molar mass.

In this work, CE-CC is applied for the first time to poly(acrylic acid) salts with different topologies, levels of branching and chain ends. The average branching structures are assessed qualitatively by solution-state NMR, to benchmark the first separation obtained by CE-CC. The aim of this paper is to separate PNaA chains according to branching and chain ends and thus to unveil the mechanism of separation occurring during the CE analysis.

Material and Methods

Materials

Water was of MilliQ quality. Boric acid (≥98%) was purchased from BHD AnalaR, Merck Pty Limited. The sodium hydroxide pellets and dimethyl sulfoxide, DMSO, were supplied by Sigma Chemical company. *Tert*-butyl acrylate (98%), acrylic acid (99%), acryloyl chloride (97%), triethylamine (≥99%), thiophenol (97%), tetrahydrofuran (THF) (≥99%) and 1,4-dioxane (≥99%) were purchased from Sigma-Aldrich. Ammonium acetate (98%) was obtained from Sharlau and the 28% ammonia solution was from Fronine Pty Ltd. Deuterated 1,4-dioxane (99%D) and deuterium oxide, D_2O (99.9%D) were supplied by Cambridge Isotope Laboratories, Inc. and 1,4-dioxane (≥99%) was from Sigma-Aldrich. Monams alkoxyamine, BlocBuilder MA alkoxyamine

and SG1 nitroxide were kindly provided by Arkema. The trifunctional alkoxyamine was prepared as described in reference [44]. The alkoxyamine MAMA-NHOH was prepared as described in references [45, 46].

Inimer alkoxyamine synthesis

MAMA-NHOH alkoxyamine (5.9 g, 13.3 mmol) and triethylamine (1.390 g, 13.7 mmol, 1.03 eq. per OH function) were dissolved in anhydrous THF (80 mL) and stirred for 10 min in an iced water bath. Acryloyl chloride (1.805 g, 19.95 mmol, 1.5 eq. per OH function) in solution in 10 mL of anhydrous THF was then added dropwise into the mixture under argon atmosphere. The mixture was stirred at room temperature for 10 h. The raw mixture was filtered and the THF evaporated. Water was then added to the residue, followed by two extractions with diethyl ether. The combined organic phases were washed with HCl (5 wt%), water and $NaHCO_3$ (5 wt%). After drying on magnesium sulfate, filtration and removal of the solvent, the oily product was dried under vacuum pump to yield the Inimer Alkoxyamine (60%). ^{1}H NMR (ppm, $CDCl_3$, 300.13 MHz): δ 1.08 (s, 9 H); 1.22 (s, 9 H); 1.30 (m, 6H) ; 1.55 (s, 3 H); 1.70 (s, 3 H); 3.35 (d, 1H, $^{1}J_{H\text{-}P}$ = 29 Hz); 3.50-4.40 (m, 8 H) ; 5.87 (d, 1H) ; 6.12 (dd, 1H) ; 6.40 (d, 1H) ; 8.36 (s, 1H). ^{31}P NMR (ppm, $CDCl_3$, 121.49 MHz): δ 27.42 (s). ^{13}C NMR (75.48 MHz, $CDCl_3$, δ, ppm): 15.9 (d, $J_{(C,P)}$ = 6.8 Hz, $POCH_2\underline{C}H_3$), 16.2 (d, $J_{(C,P)}$ = 6.0 Hz, $POCH_2\underline{C}H_3$), 23.9 (s, $\underline{C}H_3CO$), 24.7 (s, $\underline{C}H_3CO$), 29.4 (d, $J_{(C,P)}$ = 6.5 Hz, $CHC(\underline{C}H_3)_3$), 29.6 (s, $(\underline{C}H_3)_3CN$), 35.9 (d, $J_{(C,P)}$ = 8.1 Hz, $(CH_3)_3\text{–}\underline{C}\text{–}CHP$), 49.5 (s, $CONH\text{–}\underline{C}H_2\text{–}$), 59.75 (d, $J_{(C,P)}$. 8.0 Hz, $PO\underline{C}H_2$), 62.4 (s, $CH_2\underline{C}H_2O$-), 61.57 (d, $J_{(C,P)}$ .6.0 Hz, $PO\underline{C}H_2$), 62.9 (s, $N\text{–}\underline{C}(CH_3)_3$), 70.9 (d, $J_{(C,P)}$ = 133.5 Hz, CHP), 85.2 (s, $NO\text{–}\underline{C}(CH_3)_2\text{–}$), 128.2 (C=C), 130.4 (C=C), 165.6 ($\underline{C}$(=O)O) 176.6 (s, (–$\underline{C}$(=O)NH).

Polymer synthesis

Poly(sodium acrylate) (PNaA) noted as linear PNaA was bought from Polymer Standard Services (PSS, Mainz, Germany, lot number paa26027) where it had been obtained by anionic polymerization of poly(*tert*-butyl acrylate) and hydrolysis and characterized as having a number-average molar mass, M_n, and dispersity, D, of M_n = 39,300 g·mol^{-1} and D = 1.03.

The acrylic acid polymerization reactions were carried out in Schlenk tubes using 1,4-dioxane as solvent and initiated with various alkoxyamines. In a typical recipe, Monams (350 mg, 0.912 mmol), SG1 (0.024 g, 0.0821 mmol, 9 mol % with respect to Monams) and acrylic acid (10.0 g, 0.139 mol, 3.03 mol.L^{-1}) were dissolved in the solvent (1,4-dioxane, 35 mL). Then, the polymerization solution was transferred into the Schlenk tube and deoxygenated by argon bubbling for 30 min. The tube was then sealed and heated at 120 °C for 3 h. The tube was cooled, a sample was withdrawn to determine the conversion by ^{1}H NMR [10] and the polymerization mixture was precipitated into cold diethyl ether. After methylation of the carboxylic acid groups as described in [10] the various PAA were analyzed by size-exclusion chromatography (SEC) with THF as eluent. The molar masses are determined using polystyrene calibration and Mark-Houwink-Sakurada parameters, based on reference [10] for poly(acrylic acid) methylated into poly(methyl acrylate) and reference [47] for poly(t-butyl acrylate), and their accuracy is potentially affected by incomplete separation (local dispersity significantly above unity) measured in the case of hydrophobic polyacrylates [18, 20], but never investigated in case of PAA. The reaction time, conversion, M_n and D values of the different samples are given below. Exp1: NMP-PAA1

(Monams/SG1/AA/1,4-dioxane): 3 h, 72 % conv., M_n=6,900 g.mol^{-1}, D=1.34. Exp2: 3-arm star PAA (trifunctional alkoxyamine/SG1/AA/dioxane): 3 h, 65 % conv., M_n=8,500 g.mol^{-1}, D=1.6. Exp3: NMP-PtBa-1 (Monams/SG1/tBA): 3 h, 65 % conv., M_n=7500 g.mol^{-1}, D=1.2. Exp4: Hyperbranched polymer (SG1-Inimer/SG1/AA/dioxane): 3 h, 50 % conv., M_n=12,300 g.mol^{-1}, D=2.2.

The removal of the SG1 nitroxide from the chain end was performed as described in reference [48]. The hydrolysis of poly(*tert*-butyl acrylate) was performed as described in reference [49] (5 fold molar excess of trifluoroacetic acid compared to the ester moieties).

Buffers preparation

A sodium borate buffer stock solution (500 mM, 100 mL) at pH 9.2 was prepared by titrating a 500 mM aqueous boric acid solution with a 10 M sodium hydroxide aqueous solution. The 110 mM sodium borate buffer (NB110) was prepared from the respective stock solution by dilution with water. An ammonium acetate buffer stock solution (500 mM, 100 mL) at pH 9.2 was prepared by titrating a 500 mM aqueous acetic acid solution with a 28% ammonia solution. The 75 mM ammonium acetate buffer (AA75) was prepared from this stock solution by dilution with water. Each buffer was filtered with a Millipore PES membrane filter (0.2 µm) and sonicated for 5 min prior to use (with the exception of AA75). All sonication was conducted using a YJ5120-1 Ultrasonic Cleaner. Ammonium acetate buffers were stored in the freezer to avoid the evaporation of ammonia or acetic acid, while borate buffers were stored at room temperature.

Size-Exclusion Chromatography (SEC)

The SEC analyses were performed using an EcoSEC system from Tosoh equipped with a differential refractometer detector. THF was used as an eluent with 0.25 vol.% toluene as flow marker at a flow rate of 0.3 mL·min^{-1} after filtration on Alltech PTFE membranes with a porosity of 0.2 µm. The column oven was kept at 40 °C, and the injection volume was 20 µL. One ResiPore pre-column (50 mm length, 4.6 mm diameter) and two ResiPore columns (250 mm length, 4.9 mm diameter) from Polymer Laboratories were used in series. The system was calibrated using polystyrene (PS) standards the ranging from 100 to 400,000 g·mol^{-1}, purchased from Agilent.

Capillary electrophoresis (CE)

The samples (10 mg) were dissolved in water (1.5 mL) with a small volume of sodium hydroxide (15 µL, 1 mol·L^{-1}) or sodium borate (30 µL, 500 mmol·L^{-1}) added for complete dissolution and leading thus to poly(sodium acrylate) (PNaA); dimethyl sulfoxide (DMSO, 10 µL) was also added as electroosmotic flow marker. The separations were performed with a 7100 CE capillary electrophoresis system (Agilent Technologies). Capillaries were 50 µm ID fused silica capillaries (Polymicro, USA) with a 62 cm total length and a 53.5 cm effective length. The pretreatment consisted of a 10 min flush with NaOH (1 M), a 5 min flush with NaOH (0.1 M), a 5 min flush with water and a 5 min with the relevant running buffer. This treatment of the capillary was done every 5 or 6 injections. The capillary treatment between successive injections consisted of a

1 min flush with NaOH (1M) and a 5 min flush with the running buffer. The samples were injected hydrodynamically with an injection pressure of 30 mbar for 10 s, which represents an injection volume of ca 12 nL (0.24 % of the capillary volume, see calculation in the Electronic Supplementary Material, ESM). The voltage for all injections was 30 kV and the temperature 25 °C. The injections used NB110 buffer unless specified otherwise. The capillary was validated using an oligoacrylate standard of known electropherogram, AA4.[38, 39] The data was acquired using Chemstation A.10.01 software. The results analysis was conducted with the Origin 8.5.1 software. The electrophoretic mobility was calculated as in [38] and is preferred to migration time since (i) it is a reproducible quantity, (ii) it characterises the topology of the polymers[50].

NMR spectroscopy

For the quantification of the conversion, quantitative ^{1}H NMR spectra of the polymerisation media were obtained on a Bruker Avance DPX 300 spectrometer at 300 MHz (^{1}H).[10] Chemical shifts were referenced to the tetramethylsilane (TMS) signal at 0 ppm.

For the assessment of the branching structure, the hyperbranched PAA was dissolved at 50 mg mL^{-1} in deuterated 1,4-dioxane. The 3-arm star PNaA was prepared by dissolving the sample at 50 mg mL^{-1} in D_2O with 428 mM NaOH (9.25 molar equivalents to the carboxylic acid groups of PNaA). The linear sample was dissolved at 150 mg mL^{-1} in D_2O. All NMR spectra were recorded using a Bruker DRX300 spectrometer (Bruker Biospin Ltd, Sydney) equipped with a 5 mm dual 1H/13C probe, at Larmor frequencies of 300.13 MHz for ^{1}H and 75 MHz for ^{13}C, at room temperature. ^{1}H NMR spectra were recorded with a 30° flip angle, a 5 s repetition delay, and 128 scans. ^{13}C NMR spectra were recorded with inverse-gated decoupling, a 90° flip angle, a 20 s repetition delay, and 11,264 scans for hyperbranched PAA or 28,672 scans for linear PNaA and 3-arm star PNaA. These conditions should not be far from yielding quantitative spectra for the purpose of estimating the degree of branching originating in intra- and intermolecular transfer to polymer.[10] However, the samples studied have very different branching architectures and are expected to exhibit different relaxation behaviours. Therefore, it was out of the scope of this work to accurately determine conditions yielding quantitative spectra for all samples. The ^{1}H and ^{13}C chemical shift scales were externally calibrated to the methyl signal of ethanol in D_2O at 1.17 ppm and 17.47 ppm respectively.[51] All experimental data was acquired and processed using Bruker Topspin 1.3 software. The letters used for signal assignment are shown on Fig. 1 and Fig. 2a.

Results and Discussion

Different poly(sodium acrylate)s, PNaAs, were separated by capillary electrophoresis in the critical conditions, CE-CC. These samples include a linear PNaA which is expected to have a linear structure since its precursor was synthesized by anionic polymerization [7]. The other PNaAs were obtained by nitroxide-mediated polymerization of acrylic acid controlled by SG1 in dioxane,[52] with a monofunctional initiator or a trifunctional initiators or an inimer. Branching through a quaternary carbon (see Figure 1d) is expected in all these polymers (obtained by a radical polymerization process) but the initiators are designed to lead to a 3-arm star PAA in the case of the trifunctional initiator and a hyperbranched PNaA in the case of the inimer (see Fig. 1a and 1 c).

Confirmation of different branching topologies via NMR spectroscopy

Solution-state ^{1}H and ^{13}C NMR spectra of linear PNaA were consistent with published spectra of PNaAs (see Fig. S-1, Table S-1, Table S-2 in ESM and Fig. 2a, respectively). PAA synthesized by Couvreur *et al.* [10] and Loiseau *et al.* [11] showed a ^{13}C NMR chemical shift at 47.4 ppm for PAA and 48.5-50 ppm for PNaA respectively for the quaternary carbon of a branching point. Since we analyse PNaA, the quaternary carbon signal is expected around 48.5-50 ppm. There was no branching detected in the ^{13}C NMR spectrum of linear PNaA despite the high number of scans (28,672), thus confirming its linear structure.

The detection of the expected ^{1}H and ^{13}C NMR signals from the 3-arm star and hyperbranched polymers demonstrates that the expected structure was obtained for most molecules in the samples (see respectively Fig. S-2, Table S-3, Table S-4 in ESM, Fig. 2b and Fig. S-3, Table S-5, Table S-6 in ESM, Fig. 2c). Uncontrolled branching was detected through the quaternary carbon signal in the ^{13}C NMR spectra at 50 ppm (3-arm, star, signal C_q on Fig. 2b) and 48 ppm (hyperbranched, signal H on Fig. 2c). Residual dioxane from the synthesis was observed in the ^{1}H and ^{13}C NMR spectra of the 3-arm star polymer (Fig. S-2 in ESM and Fig. 2b). Residual acrylic double bonds from the synthesis was observed in the ^{1}H and ^{13}C NMR spectra (respectively Fig. S-2 in ESM and Fig. 2b for the 3-arm star and Fig. S-3 in ESM and Fig. 2b for the hyperbranched). In the 3-arm star, the double bonds could originate in unreacted acrylic acid and/or in macromonomer formed by beta-scission after transfer to the polymer at moderate temperature [53]. Closer examination of the ^{1}H NMR spectrum (Fig. S-2b in ESM) reveals the exact splitting pattern of unreacted acrylic acid (three doublets of doublets), disproving the presence of macromonomer in significant proportion in the 3-arm star. In the hyperbranched polymer, the double bonds could also originate in the unsaturated chain end of the hyperbranched polymer (Fig. 1c). Closer examination of the ^{1}H NMR spectrum (Fig. S-3b in ESM) reveals the exact splitting pattern of the unsaturated chain end of the hyperbranched polymer or of the unreacted acrylic acid, disproving the presence of macromonomer from beta-scission in significant proportion. Furthermore, both ^{1}H and ^{13}C NMR spectra indicate the presence of one of these species only (exact ^{1}H splitting pattern, single set of three ^{13}C NMR signals), indicating that the double bonds are from the unsaturated chain end of the hyperbranched polymer (Fig. 1c).

Separation according to the topology

Separation according to different branching topologies of PNaA were observed for the first time using CE-CC. The hyperbranched, 3-arm star and linear PNaAs were separated within 15 minutes (Fig. 3a). This separation is faster than other separation methods for PAA like SEC and LC-CC.[17, 24, 31] The separation is counter-electroosmotic flow with a positive electroosmotic flow and a negative electrophoretic mobility (Fig. S-4 in ESM). Variations of electroosmotic flow are larger than the variations of electrophoretic mobility. In this work, only electrophoretic mobilities distributions are thus presented from Fig. 3b onward. The electrophoretic mobility is calculated as shown in Equation (1) of the ESM. The hyperbranched PNaA exhibits the lowest electrophoretic mobility followed by the 3-arm star and linear PNaA respectively (Fig. 3b). The lowest degree of polymerization is expected to be the one of the 3-arm star with a degree of polymerization of 118. The

electrophoretic mobility is expected at these degrees of polymerization to slightly decrease with degree of polymerization [37]. It is in fact to note that the degree of polymerization increase from 3-arm star (118) to hyperbranched (171) and finally linear PNaA (545). If the degree of polymerization was significantly influencing the electrophoretic mobilities in this work, these mobilities would be the highest for 3-arm star, followed closely by hyperbranched PNaA and finally a somehow lower value for the linear. This is not the observed order of migration and the effect of degree of polymerisation is negligible with these PNaA with degree of polymerization above 100. The electrophoretic mobility increases as the degree of branching decreases. The same behaviour was observed in the case of the two components of starch: the hyperbranched amylopectin has a lower mobility than the slightly (long-chain) branched amylose.[54] The PNaAs are separated at pH 9.2, ca 3 units of pH above the pKa of their carboxylic acid moieties. The differences in electrophoretic mobilities with branching can be understood as a decrease of effective charge of the PNaAs with the branching as demonstrated recently in the case of dendrigraft using isotachophoresis [43].

The variation of the electrophoretic mobility with branching is the key to the separation by branching we propose in this work. The different samples are not completely separated, partially because the topology (i.e., the distribution of degrees of branching or distribution of molar masses of the branches) is not controlled. Thus the samples are not expected to contain each a unique branched structure, different from that of the other samples, and that could be fully resolved one from one another. It is however important to show that the difference of electrophoretic mobilities from sample to sample are significant. A high repeatability of the electrophoretic mobility taken as the maximum of the electrophoretic mobility distribution, was observed for the separation of linear ($n \geq 9$) and hyperbranched ($n \geq 7$) PNaA with a relative standard deviation (RSD) value lower than 2.41 % and 1.45 % respectively (See Table 1 and Table S-7). The accuracy of the electrophoretic mobilities of the linear, 3-arm star and hyperbranched PNaA in CE-CC was assessed by reproducing their separation with a different operator and different capillary. Highly reproducible mobilities were observed with a RSD value below 1.63 %: 1.63 % for the linear PNaA ($n = 23$), 1.34 % for the 3-arm star PNaA ($n = 17$) and 1.15% for the hyperbranched PNaA ($n = 19$) (Table 1). Although the differences in electrophoretic mobilities between the different samples are not large, they are significant (the differences in electrophoretic mobilities at the maximum of the distribution are larger than the standard deviation obtained even in a reproducibility test). The relatively small differences in electrophoretic mobilities with topology reflect not only the selectivity but also the intrinsic complexity of these samples including at least 1000s of molecules differing by their molar mass or their degree of branching or the position of their branching points or the distribution of molar masses of their branches. It is to be noted that in comparison, round-robin tests on SEC of PAA indicated variations of several hundred percents of their determined average molar masses.[55]

The electrophoretic mobility of polyelectrolytes changes with the nature of the counter-ion and the electrolyte they migrate in.[38] Linear, 3-arm star and hyperbranched poly(ammonium acrylate)s were also separated using ammonium acetate (AA75) as a buffer. While the mobilities values were different, the migration order was the same (see Table 1 and Fig. S-5 in ESM) confirming the reproducibility and robustness of the separation by topology of PAA salts using CE-CC.

Homogeneity of the branching topology

The hyperbranched and 3-arm star polymers both exhibit a main electrophoretic mobility distribution that is discussed in the previous paragraph but also an underlying broader electrophoretic mobility distribution. These samples are expected to have a controlled branching structure (due to the structure of the initiator), with an underlying uncontrolled one arising from transfer to polymer. PNaA with branching only arising from transfer to polymer (monofunctional initiator, namely Monams) [10] have also been injected: either PNaA obtained from NMP of AA (sample NMP-PAA1) or PNaA obtained from NMP of *tert*-butyl acrylate and hydrolysis (NMP-PtBA1). NMP of AA also leads to a bimodal distribution: a relatively narrow electrophoretic mobility distribution with an underlying broad one. Only the broad electrophoretic mobility distribution is observed with the PNaA obtained from NMP of *tert*-butyl acrylate (see Fig. S-6 and the solid line curves on Fig. 4). The broad distribution is attributed to the broad range of topologies obtained by radical polymerization and involving transfers to polymer. CE-CC can thus probe the homogeneity of the branching in a polyelectrolyte sample. CE-CC is expected to be sensitive to low levels of long branches in the sample at levels that NMR may not be sensitive enough to detect.

Separation of PNaAs according to their chain end

LC-CC separates polymers according to their topology as well as their end groups, including SG1 end groups,[23] but no separation by end groups has ever been published for PAA or one its salts. Free solution CE was shown to separate polypeptides according to their end-groups.[56] The separation of PNaAs differing only by their end groups was also investigated by CE-CC in this work. The end group for NMP-PNAA1 was a SG1 moiety. Some NMP-PAA1 was heated in the presence of thiophenol to replace the SG1 end group by a hydrogen as in [48], yielding NMP-PAA2. The electrophoretic mobility decreased significantly after the end-group modification (see Fig. 4a and Fig. S-6 in ESM). This is expected since the neutral and bulky SG1 moiety was adding only to the friction of the PNaA, not to its charge, and it should be replaced simply by a hydrogen atom. NMP-PAA1 exhibits a bimodal electrophoretic mobility distribution with a relatively narrow distribution superimposing on a broader distribution. After thiophenol treatment, the broader distribution is shifting by ca 0.1×10^{-8} $m^2 \cdot V^{-1} \cdot s^{-1}$, while the narrower distribution shift by less than 0.05×10^{-8} $m^2 \cdot V^{-1} \cdot s^{-1}$. This difference may be explained either by difference in end-groups between the two populations of by difference in topologies. The narrower distribution might correspond to PNaA chains bearing one SG1 end-group, while the broader one might correspond to PNaA chains bearing several SG1 end-groups, possible because of the redistribution of SG1 end-group due to intermolecular chain transfer to polymer. Another, more likely, explanation is that the NMP-PAA2 is more heterogeneous in terms of topology than NMP-PAA1 due to potential hydrogen abstraction reactions followed by termination by combination of β-scission reaction when the PAA is exposed to 120 °C (the expected reaction is the transfer to thiophenol, but the occurrence of these side reactions is also likely although their extent is unknown). The side reactions occurring during thiophenol treatment would also explain the decrease of the relative intensity of the narrower mobility distributions compared to the broad one, indicating a more heterogeneous material in terms of branching. This study of end-group is particularly relevant since the SG1 group allows reinitiation of the polymerization needed to create block copolymer and functionalize further the polymer: the presence of SG1 as end group is characteristic of a living chain,[13] while NMP-PAA2

contains only “dead” chains. Considering that NMP-PAA1 chains with electrophoretic mobility above 3.57 $m^2 \cdot V^{-1} \cdot s^{-1}$ are dead chains (based on NMP-PAA2 mobilites), then NMP-PAA1 would contain ca 69 % living chains.

The thiophenol treatment was also applied to some of the hydrolysed sample NMP-PtBA1. There was no significant difference in electrophoretic mobility between hydrolysed NMP-PtBA1 and NMP-PtBA2 (Fig. 4b). This indicates that the thiophenol treatment does not affect NMP-PtBA1. It is to note that NMP-PtBA1 and NMP-PtBA2 mobility distributions are broader than the ones observed for NMP-PAA1. The hydrolysis with TFA leading to PtBA1 may hydrolyze selectively the *tert*-butyl groups of the SG1 moieties in this polymer as expected from previous mass spectrometric analysis [57]. The molar ratio of TFA to SG1 chain ends is 6 to 17 times higher in this work than in the previous mass spectrometric analysis (see Table S-8, ESM). TFA is however also consumed by *tert*-butyl group on the acrylate monomer unit (stoichiometry 1:5 for *tert*-butyl acrylate monomer unit to TFA). In our work, the SG1 end-group might have degraded during the TFA hydrolysis into a variety of end-groups, thus leading to broader electrophoretic mobility distributions. These end-groups are then not thermosensitive and the thiophenol treatment does not significantly modify NMP-PtBA1 end-groups or topology.

Conclusions

First time separation of PNaA by topology was obtained using free-solution capillary electrophoresis, with a separation independent of molar mass corresponding to capillary electrophoresis in the critical conditions, CE-CC. CE-CC allows a precise (repeatable) determination of the electrophoretic mobility as SEC does for molar mass, but the accuracy (reproducibility) of the electrophoretic mobility of PNaA is order of magnitudes higher than the accuracy of the molar masses of PAA determined by current SEC methods. The separation of poly(acrylic acid) salts with CE-CC was benchmarked once by an assessment of the branching structures by solution-state NMR. The electrophoretic mobility of PNaA decreases with branching and CE-CC enables to probe the heterogeneity of the topology of the PNaA chains: the use of a trifunctional initiator or an inimer leads to a more homogenous branched structure, with still a broad underlying distribution of PNaA chains with various degrees of branching, branching point locations and distribution of molar masses of branches. CE-CC also separates PNaAs with different chain ends, with or without the SG1 moiety, which means that CE-CC can be used to investigate the livingness of NMP (i.e. the ability to synthesize block copolymers or functionalize PAAs). This separation applies to other branched polyelectrolyte as pioneered by the group of Cottet on dendrigaft polylysines.[43] The separation by branching using CE-CC may be highly valuable to investigate the SEC separation. SEC of branched polymers (especially branched hydrophobic polyacrylates) was shown to be influenced strongly by branching [18]: local dispersities significantly above unity were measured for poly(methyl acrylate),[19] poly(ethyl acrylate)[7], poly(n-butyl acrylate),[7, 20] poly(2-ethyl hexyl acrylate) [19, 20]. This however requires use of multiple detector which is relatively tedious and time-consuming. Coupling SEC to CE-CC [58] may enable estimating the local dispersity with higher throughput and greater ease than using viscometric and light scattering detection. The CE-CC method will also be extended other polyelectrolytes presenting a distribution of one molecular attribute: the branching structure, the chain ends, or the composition.

Acknowledgements

YG, JRAW and PC thank University of Western Sydney (UWS) – International Research Initiative Scheme for funding; MG and PC thank UWS School of Science and Health for a Seed grant. AM would like to thank UWS for granting an Australian Postgraduate Award (APA) scholarship.

References

1. Buchholtz FL (2000) Polyacrylamides and Poly(Acrylic Acids), Ullmann´s Encyclopedia of Industrial Chemistry, Wiley-VCH Verlag GmbH & Co. KGaA, Weinheim, Germany.
2. Wallace AD, Al-Hamzah A, East CP, Doherty WOS, Fellows CM (2010) Effect of Poly(acrylic acid) End-Group Functionality on Inhibition of Calcium Oxalate Crystal Growth. J. Appl. Polym. Sci. 116:1165-1171
3. East CP, Wallace AD, Al-Hamzah A, Doherty WOS, Fellows CM (2010) Effect of Poly(acrylic acid) Molecular Mass and End-Group Functionality on Calcium Oxalate Crystal Morphology and Growth. J. Appl. Polym. Sci. 115:2127-2135
4. Duan SF, Cai S, Xie YM, Bagby T, Ren SQ, Forrest ML (2012) Synthesis and Characterization of a Multiarm Poly(acrylic acid) Star Polymer for Application in Sustained Delivery of Cisplatin and a Nitric Oxide Prodrug. J. Polym. Sci. Pol. Chem. 50:2715-2724
5. Asua JM, Beuermann S, Buback M, Castignolles P, Charleux B, Gilbert RG, Hutchinson RA, Leiza JR, Nikitin AN, Vairon JP, van Herk AM (2004) Critically evaluated rate coefficients for free-radical polymerization, 5 - Propagation rate coefficient for butyl acrylate. Macromol. Chem. Phys. 205:2151-2160
6. Junkers T, Barner-Kowollik C (2008) The Role of Mid-Chain Radicals in Acrylate Free Radical Polymerization: Branching and Scission. J. Polym. Sci. Polym. Chem. 46:7585-7605
7. Gaborieau M, Nicolas J, Save M, Charleux B, Vairon J-P, Gilbert RG, Castignolles P (2008) Multiple-detection size-exclusion chromatography of complex branched polyacrylates. J. Chromatogr. A 1190:215-233
8. Farcet C, Belleney J, Charleux B, Pirri R (2002) Structural characterization of nitroxide-terminated poly(n-butyl acrylate) prepared in bulk and miniemulsion polymerizations. Macromolecules 35:4912-4918
9. Buback M, Hesse P, Lacik I (2007) Propagation rate coefficient and fraction of mid-chain radicals for acrylic acid polymerization in aqueous solution. Macromol. Rapid Commun. 28:2049-2054
10. Couvreur L, Lefay C, Belleney J, Charleux B, Guerret O, Magnet S (2003) First Nitroxide-Mediated Controlled Free-Radical Polymerization of Acrylic Acid. Macromolecules 36:8260-8267
11. Loiseau J, Doerr N, Suau JM, Egraz JB, Llauro MF, Ladaviere C (2003) Synthesis and characterization of poly(acrylic acid) produced by RAFT polymerization. Application as a very efficient dispersant of CaCO3, kaolin, and TiO2. Macromolecules 36:3066-3077
12. Hawker CJ, Frechet JMJ, Grubbs RB, Dao J (1995) Preparation of hyperbranched and star polymers by a living, self-condensing free-radical polymerization. J. Am. Chem. Soc. 117:10763-10764
13. Nicolas J, Guillaneuf Y, Lefay C, Bertin D, Gigmes D, Charleux B (2013) Nitroxide-mediated polymerization. Prog. Polym. Sci. 38:63-235
14. Castignolles P, Graf R, Parkinson M, Wilhelm M, Gaborieau M (2009) Detection and quantification of branching in polyacrylates by size-exclusion chromatography (SEC) and melt-state 13C NMR spectroscopy. Polymer 50:2373-2383

15. Ahmad NM, Charleux B, Farcet C, Ferguson CJ, Gaynor SG, Hawkett BS, Heatley F, Klumperman B, Konkolewicz D, Lovell PA, Matyjaszewski K, Venkatesh R (2009) Chain Transfer to Polymer and Branching in Controlled Radical Polymerizations of n-Butyl Acrylate. Macromol. Rapid Commun. 30:2002-2021
16. Gaborieau M, Koo SPS, Castignolles P, Junkers T, Barner-Kowollik C (2010) Reducing the degree of branching in polyacrylates via midchain radical patching: a quantitative melt-state NMR study. Macromolecules 43:5492–5495
17. Lacik I, Beuermann S, Buback M (2001) Aqueous phase size-exclusion-chromatography used for PLP-SEC studies into free-radical propagation rate of acrylic acid in aqueous solution. Macromolecules 34:6224-6228
18. Gaborieau M, Castignolles P (2011) Size-exclusion chromatography (SEC) of branched polymers and polysaccharides. Anal. Bioanal. Chem. 399:1413-1423
19. Junkers T, Schneider-Baumann M, Koo SSP, Castignolles P, Barner-Kowollik C (2010) Determination of Propagation Rate Coefficients for Methyl and 2-Ethylhexyl Acrylate via High Frequency PLP−SEC under Consideration of the Impact of Chain Branching. Macromolecules 43:10427-10434
20. Castignolles P (2009) Transfer to Polymer and Long-Chain Branching in PLP-SEC of Acrylates. Macromol. Rapid Commun. 30: 1995 - 2001
21. Olesik SV (2004) Liquid chromatography at the critical condition. Anal. Bioanal. Chem. 378:43-45
22. Berek D (2008) Separation of parent homopolymers from diblock copolymers by liquid chromatography under limiting conditions desorption, 1 - Principle of the method. Macromol. Chem. Phys. 209:695-706
23. Rollet M, Gle D, Phan TNT, Guillaneuf Y, Bertin D, Gigmes D (2012) Characterization of Functional Poly(ethylene oxide)s and Their Corresponding Polystyrene Block Copolymers by Liquid Chromatography under Critical Conditions in Organic Solvents. Macromolecules 45:7171-7178
24. Phillips SL, Olesik SV (2003) Initial characterization of humic acids using liquid chromatography at the critical condition followed by size-exclusion chromatography and electrospray ionization mass spectrometry. Anal. Chem. 75:5544-5553
25. Mass V, Bellas V, Pasch H (2008) Two-Dimensional Chromatography of Complex Polymers, 7-Detailed Study of Polystyrene-block-Polyisoprene Diblock Copolymers Prepared by Sequential Anionic Polymerization and Coupling Chemistry. Macromol. Chem. Phys. 209:2026-2039
26. Im K, Park H-W, Kim Y, Ahn S, Chang T, Lee K, Lee H-J, Ziebarth J, Wang Y (2008) Retention Behavior of Star-Shaped Polystyrene near the Chromatographic Critical Condition. Macromolecules 41:3375-3383
27. Beaudoin E, Favier A, Galindo C, Lapp A, Petit C, Gigmes D, Marque S, Bertin D (2008) Reduced sample recovery in liquid chromatography at critical adsorption point of high molar mass polystyrene. Eur. Polym. J. 44:514-522
28. Jacquin M, Muller P, Lizarraga G, Bauer C, Cottet H, Theodoly O (2007) Characterization of amphiphilic diblock copolymers synthesized by MADIX polymerization process. Macromolecules 40:2672-2682
29. Favier A, Petit C, Beaudoin E, Bertin D (2009) Liquid chromatography at the critical adsorption point (LC-CAP) of high molecular weight polystyrene: pushing back the limits of reduced sample recovery. e-Polymers15
30. Pasch H, Adler M, Knecht D, Rittig F, Lange R (2006) New chromatographic and hyphenated techniques for hydrophilic copolymers. Macromol. Symp. 231:166-177
31. Phillips SL, Ding L, Stegemiller M, Olesik SV (2003) Development of water-based liquid chromatography at the critical condition. Anal. Chem. 75:5539-5543

32. Engelhardt H, Martin M (2004) Characterization of synthetic polyelectrolytes by capillary electrophoretic methods, Polyelectrolytes with Defined Molecular Architecture I, Springer-Verlag Berlin, Berlin, pp. 211-247.
33. Guillaneuf Y, Castignolles P (2008) Using apparent Molecular Weight from SEC in controlled/living polymerization and kinetics of polymerization. J. Polym. Sci. A Polym. Chem. 46:897-911
34. Cottet H, Gareil P (2008) Separation of synthetic (Co)polymers by capillary electrophoresis techniques. Methods Mol. Biol. (Totowa, NJ, U. S.) 384:541-567
35. Cottet H, Simo C, Vayaboury W, Cifuentes A (2005) Nonaqueous and aqueous capillary electrophoresis of synthetic polymers. J. Chromatogr. A 1068:59-73
36. Hoagland DA, Smisek DL, Chen DY (1996) Gel and free solution electrophoresis of variably charged polymers. Electrophoresis 17:1151-1160
37. Cottet H, Gareil P, Theodoly O, Williams CE (2000) A semi-empirical approach to the modeling of the electrophoretic mobility in free solution: Application to polystyrenesulfonates of various sulfonation rates. Electrophoresis 21:3529-3540
38. Castignolles P, Gaborieau M, Hilder EF, Sprong E, Ferguson CJ, Gilbert RG (2006) High-resolution separation of oligo(acrylic acid) by capillary zone electrophoresis. Macromol. Rapid Commun. 27:42-46
39. Gaborieau M, Causon TJ, Guillaneuf Y, Hilder EF, Castignolles P (2010) Molecular weight and tacticty of oligoacrylates by capillary electrophoresis - mass spectrometry. Aus. J. Chem. 63:1219-1226
40. Cottet H, Gareil P (2000) From small charged molecules to oligomers: A semiempirical approach to the modeling of actual mobility in free solution. Electrophoresis 21:1493-1504
41. Stellwagen NC, Gelfi C, Righetti PG (1997) The free solution mobility of DNA. Biopolymers 42:687-703
42. Taylor DL, Ferris CJ, Maniego AR, Castignolles P, in het Panhuis M, Gaborieau M (2012) Characterization of Gellan Gum by Capillary Electrophoresis. Aus. J. Chem. 65:1156-1164
43. Ibrahim A, Koval D, Kasicka V, Faye C, Cottet H (2013) Effective Charge Determination of Dendrigraft Poly-L-lysine by Capillary Isotachophoresis. Macromolecules 46:533-540
44. Dufils PE, Chagneux N, Gigmes D, Trimaille T, Marque SRA, Bertin D, Tordo P (2007) Intermolecular radical addition of alkoxyamines onto olefins: An easy access to advanced macromolecular architectures. Polymer 48:5219-5225
45. Chagneux N, Trimaille T, Rollet M, Beaudoin E, Gerard P, Bertin D, Gigmes D (2009) Synthesis of Poly(n-butyl acrylate)-b-poly(epsilon-caprolactone) through Combination of SG1 Nitroxide-Mediated Polymerization and Sn(Oct)(2)-Catalyzed Ring-Opening Polymerization: Study of Sequential and One-Step Approaches from a Dual Initiator. Macromolecules 42:9435-9442
46. Vinas J, Chagneux N, Gigmes D, Trimaille T, Favier A, Bertin D (2008) SG1-based alkoxyamine bearing a N-succinimidyl ester: A versatile tool for advanced polymer synthesis. Polymer 49:3639-3647
47. Gruendling T, Junkers T, Guilhaus M, Barner-Kowollik C (2010) Mark-Houwink Parameters for the Universal Calibration of Acrylate, Methacrylate and Vinyl Acetate Polymers Determined by Online Size-Exclusion Chromatography-Mass Spectrometry. Macromol. Chem. Phys. 211:520-528
48. Petit C, Luneau B, Beaudoin E, Gigmes D, Bertin D (2007) Liquid chromatography at the critical conditions in pure eluent: An efficient tool for the characterization of functional polystyrenes. J. Chromatogr. A 1163:128-137
49. Burguiere C, Pascual S, Bui C, Vairon JP, Charleux B, Davis KA, Matyjaszewski K, Betremieux I (2001) Block copolymers of poly(styrene) and poly(acrylic acid) of various molar masses, topologies, and compositions prepared via controlled/living radical polymerization. Application as stabilizers in emulsion polymerization. Macromolecules 34:4439-4450

50. Ibrahim A, Allison SA, Cottet H (2012) Extracting Information from the Ionic Strength Dependence of Electrophoretic Mobility by Use of the Slope Plot. Anal. Chem. 84:9422-9430
51. Gottlieb HE, Kotlyar V, Nudelman A (1997) NMR chemical shifts of common laboratory solvents as trace impurities. J. Org. Chem. 62:7512-7515
52. Lefay C, Belleney J, Charleux B, Guerret O, Magnet S (2004) End-group characterization of poly(acrylic acid) prepared by nitroxide-mediated controlled free-radical polymerization. Macromol. Rapid Commun. 25:1215-1220
53. Guillaneuf Y, Gigmes D, Junkers T (2012) Investigation of the End Group Fidelity at High Conversion during Nitroxide-Mediated Acrylate Polymerizations. Macromolecules 45:5371-5378
54. Herrero-Martinez JM, Schoenmakers PJ, Kok WT (2004) Determination of the amylose-amylopectin ratio of starches by iodine-affinity capillary electrophoresis. J. Chromatogr. A 1053:227-234
55. Berek D, Bruessau R, Lilge D, Mingozzi T, Podzimek S, Robert E, Poster: Repeatability and apparent reproducibility of molar mass values for homopolymers determined by size exclusion chromatography. in: http://old.iupac.org/projects/posters01/berek01.pdf, (Ed.), IUPAC congress/ general assembly, July 2001.
56. Souaid E, Cottet H (2005) Separation of living and dead polymers in synthetic polypeptide mixtures by nonaqueous capillary electrophoresis using differences in ionization states. Electrophoresis 26:3300-3306
57. Barrere C, Chendo C, Phan TNT, Monnier V, Trimaille T, Humbel S, Viel S, Gigmes D, Charles L (2012) Successful MALDI-MS Analysis of Synthetic Polymers with Labile End-Groups: The Case of Nitroxide-Mediated Polymerization Using the MAMA-SG1 Alkoxyamine. Chem. Eur. J. 18:7916-7924
58. Oudhoff KA, Ab Buijtenhuijs FA, Wijnen PH, Schoenmakers PJ, Kok WT (2004) Determination of the degree of substitution and its distribution of carboxymethylcelluloses by capillary zone electrophoresis. Carbohydr. Res. 339:1917-1924

Table 1 Average electrophoretic mobilities m_{ep} (10^{-8} $m^2 \cdot V^{-1} \cdot s^{-1}$) of linear, 3-arm star and hyperbranched PNaA as well as their relative standard deviations (RSD). All measured values are listed in Table S-7 in ESM. A and B are the two different operators

	Linear PNaA		**3-Arm star PNaA**		**Hyperbranched PNaA**	
	$m_{ep,A}$	$m_{ep,B}$	$m_{ep,A}$	$m_{ep,B}$	$m_{ep,A}$	$m_{ep,B}$
Average	3.61	3.58	3.51	3.53	3.53	3.49
Overall Average	3.59		3.53		3.50	
SD	0.09	0.03	n/a	0.05	0.05	0.03
Overall SD	0.06		0.05		0.04	
RSD (%)	2.41	0.76	n/a	1.46	1.45	0.79
Overall RSD (%)	1.63		1.34		1.15	

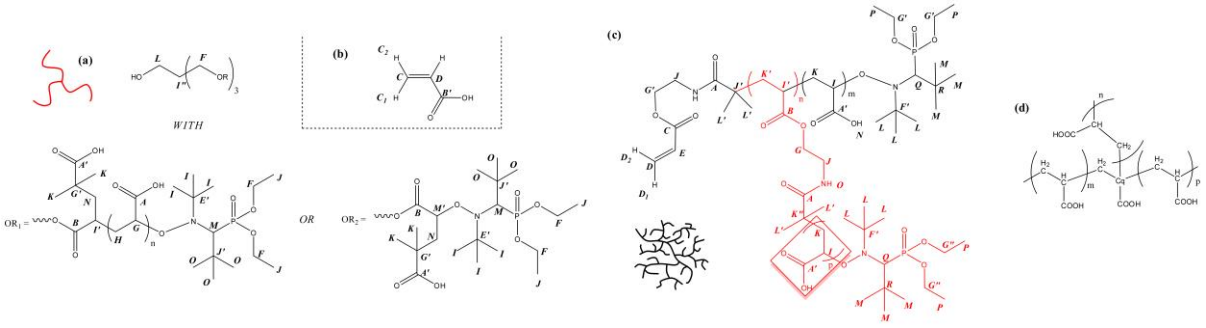

Fig. 1 Chemical structures of (a) 3-arm star PNaA, (b) acrylic acid and (c) hyperbranched PAA with letters used for the assignment of their ^{1}H NMR and ^{13}C NMR chemical shifts. Quaternary carbon C_q at the branching point resulting from transfer to polymer followed by reinitiation (d). The 3-arm star PNaA shows three R groups, each of which can be either R_1 = reacted 3-arm star PNaA or R_2 = the unreacted initiator, alcoxtriacrylate. The boxed region of the hyperbranched PAA actually consists of an equivalent of the whole red region of the molecule, which in turns contains another boxed repeat unit, actually consisting of an equivalent of the whole red region, etc., resulting in the hyperbranched structure

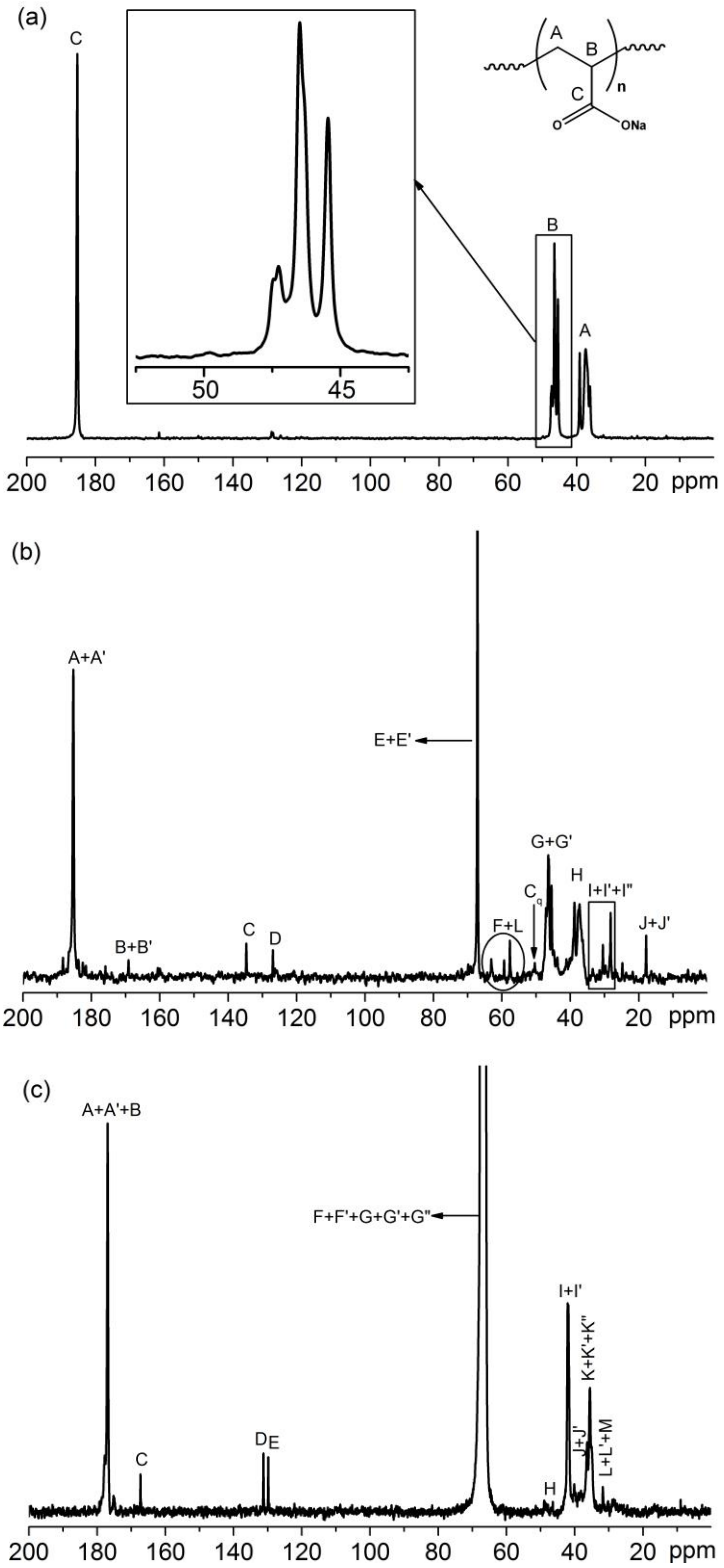

Fig. 2 ^{13}C NMR spectra of (a) linear PAA in D_2O, (b) 3-arm star PNaA in D_2O with NaOH, (c) hyperbranched PAA in 1,4-dioxane-d_8. The insert in (a) show the absence of a potential quaternary carbon signal at about 48 ppm

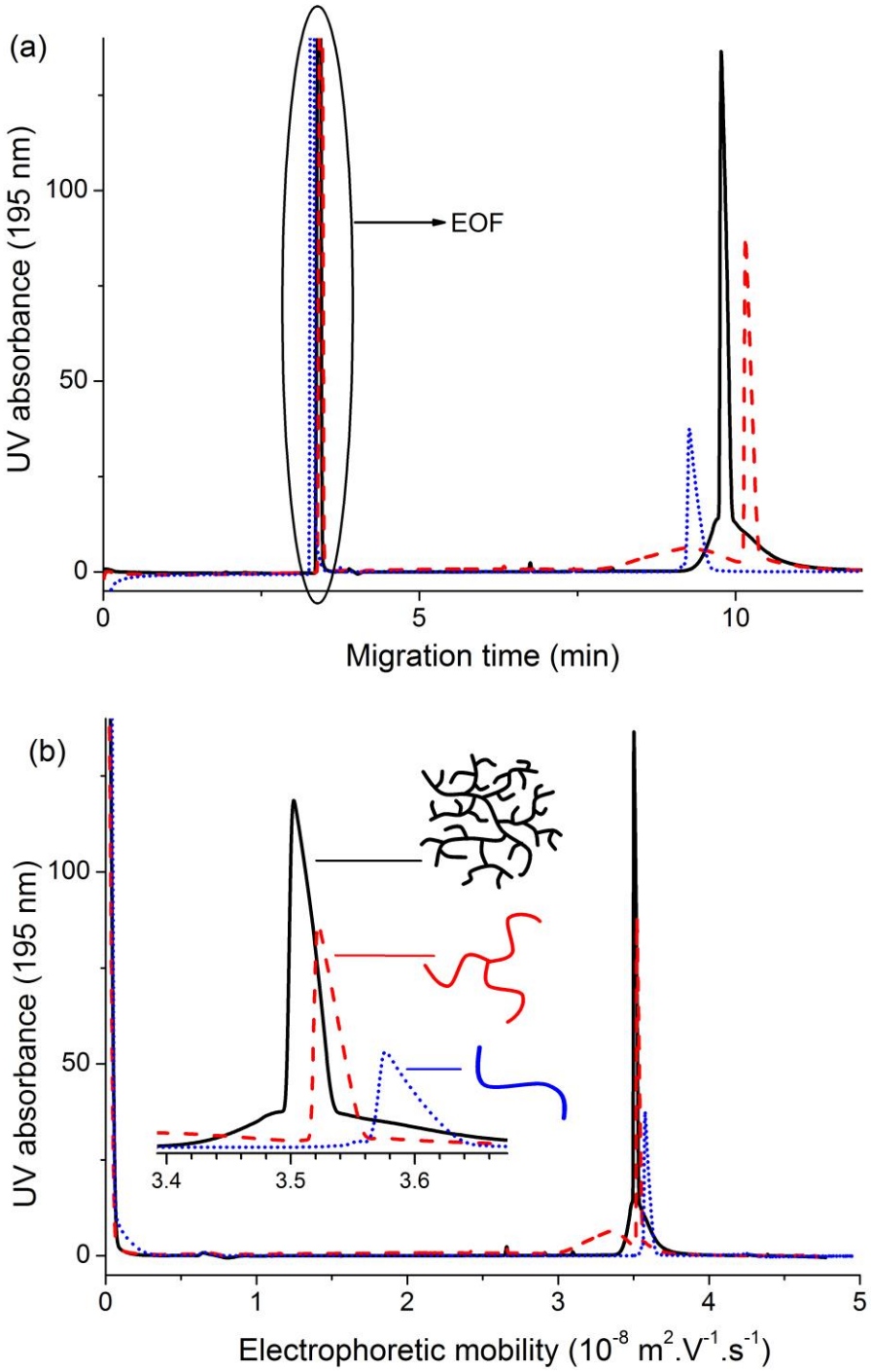

Fig. 3 Separation of linear (blue dotted line), 3-arm star (red dashed line) and hyperbranched (black solid line) PNaA by capillary electrophoresis in NB110 shown as a function of (a) migration time and (b) electrophoretic mobility, which is a more reproducible quantity than the former. The standard deviations corresponding to the repeatability and the reproducibility of the separation as a function of electrophoretic mobility are shown in Table 1

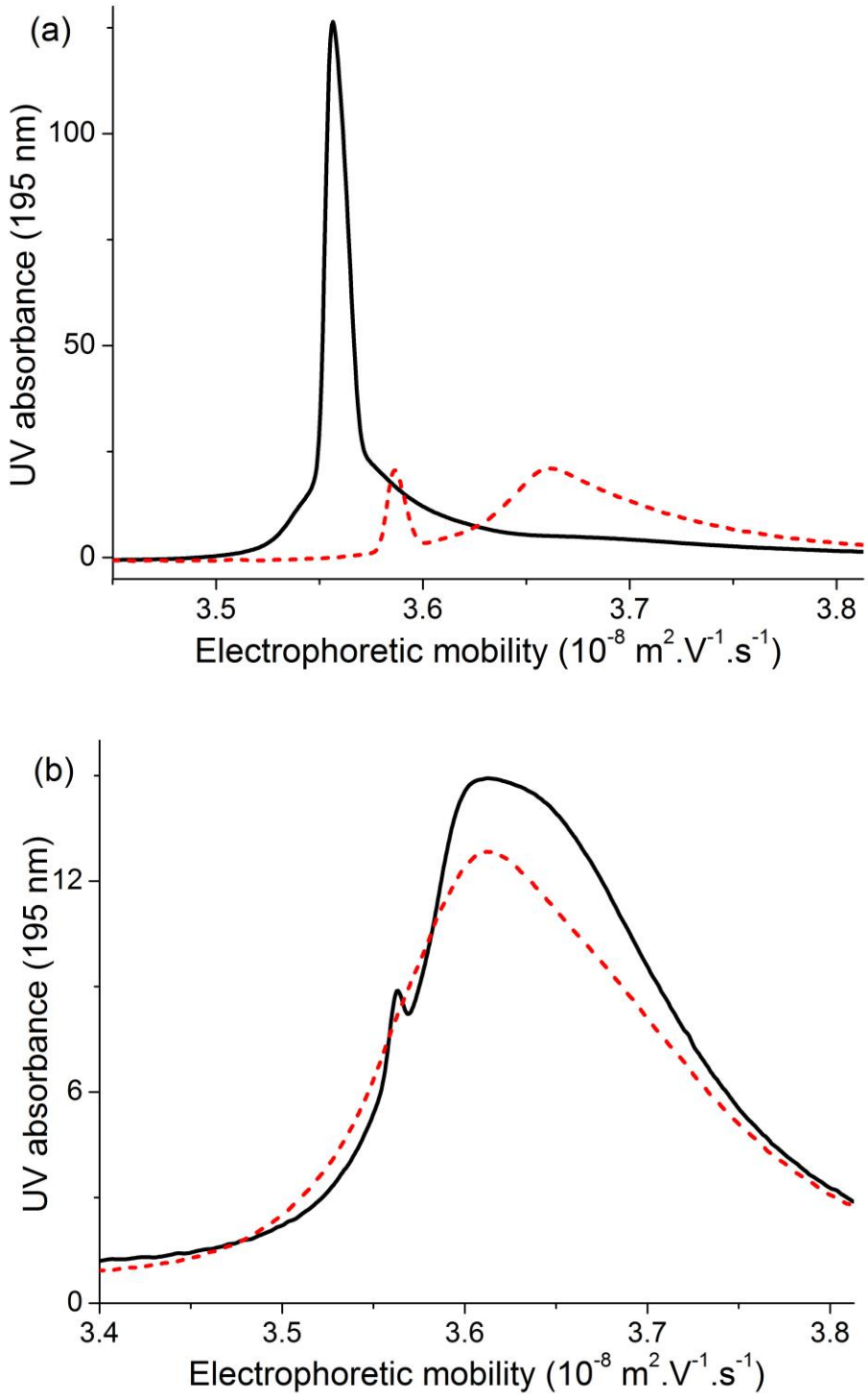

Fig. 4 Electrophoretic mobility distributions of (a) PNaA obtained by nitroxide-mediated polymerization of acrylic acid initiated by the monofunctional initiator Monams (sample NMP-PAA1, black solid line) followed by cleavage of the SG1 end-group by treatment with thiophenol (sample NMP-PAA2, red dashed line), as well as of (b) PNaA obtained by nitroxide mediated polymerization of *tert*-butyl acrylate initiated by the monofunctional initiator Monams followed by cleavage of the tBA side group by TFA hydrolysis (sample NMP-PtBA1, black solid line), followed by the same thiophenol treatment as above (sample NMP-PtBA2, red dashed line)

Online Abstract Figure

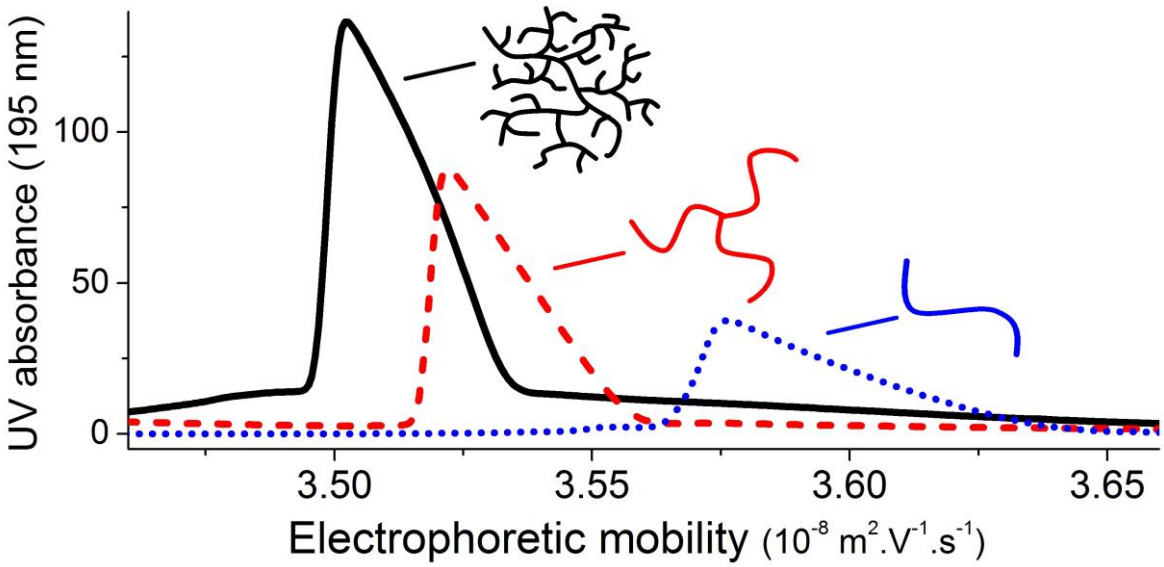

Electronic Supplementary Material

by

Alison R. Maniego,[1,2] Dale Ang,[1,2] Yohann Guillaneuf,[*,3] Catherine Lefay,[3] Didier Gigmes,[3]

Janice R. Aldrich-Wright,[2] Marianne Gaborieau,[2] Patrice Castignolles[1,*]

for

Separation of poly(acrylic acid) salts according to the topology using capillary electrophoresis in the critical conditions

[1] University of Western Sydney (UWS), Australian Centre for Research on Separation Sciences (ACROSS), School of Science and Health, Parramatta campus, Locked Bag 1797, Penrith NSW 2751, Australia

[2] University of Western Sydney (UWS), School of Science and Health, Nanoscale Organisation and Dynamics group, Locked Bag 1797, Penrith NSW 2751, Australia

[3] Aix-Marseille Université, CNRS, Institut de Chimie Radicalaire, UMR 7273, 13397, Marseille, France

* Corresponding author: p.castignolles@uws.edu.au, phone +61 2 9685 9970, fax +61 2 9685 99

This file contains:

- ^{1}H NMR spectra corresponding to ^{13}C NMR spectra presented in the main text and their peak assignment as well as the assignment of ^{13}C spectra.

- A scheme representing a counter-electroosmotic flow free-solution capillary electrophoresis separation, the equations used to calculate injection volume and electrophoretic mobility as well as the electrophoretic mobility values determined in this work and supplementary electropherograms and the ratio of trifluoroacetate used in this work and the literature for hydrolysis.

NMR spectroscopy

The hydrogens of the secondary and tertiary carbon for the monomer unit in PNaA were detected at 1.7 and 2.1 ppm, respectively (Figure S-1). The ^{1}H in the carboxylic group and residual moisture react with D_2O resulting in a HOD peak at 4.9. The small signal observed at 7.2 ppm could be residual solvent from the synthesis (by anionic polymerization, which may be toluene). The ^{13}C NMR spectrum confirmed the chemical structure of the linear PNaA with the detection of the CH and CH_2 groups of the main chain of PNaA, as well as the carboxylic acid carbon (Figure 1). It confirmed the sample to be the conjugated base of PAA which is PNaA. The is due to a higher chemical shifts observed in this spectrum in comparison to the ^{13}C NMR spectrum of a nitroxide-mediated polymerised PAA by Couvreur *et al.*.[1] Higher chemical shifts were observed for PAA as the pD of D_2O becomes more alkaline.[2] No signal of quaternary carbon was detected around 48-50 ppm (Fig. 2a): the weak increase in the baseline at about 50 ppm has a signal-to-noise ratio of 2.7, which is not significant (after 28,672 scans, noise level measured over 70-60 ppm range).

The ^{1}H and ^{13}C NMR chemical shift assignments of the linear PAA are listed in Table S-1 and S-2, respectively. Letters refer to the molecular structure shown on Figure 1.

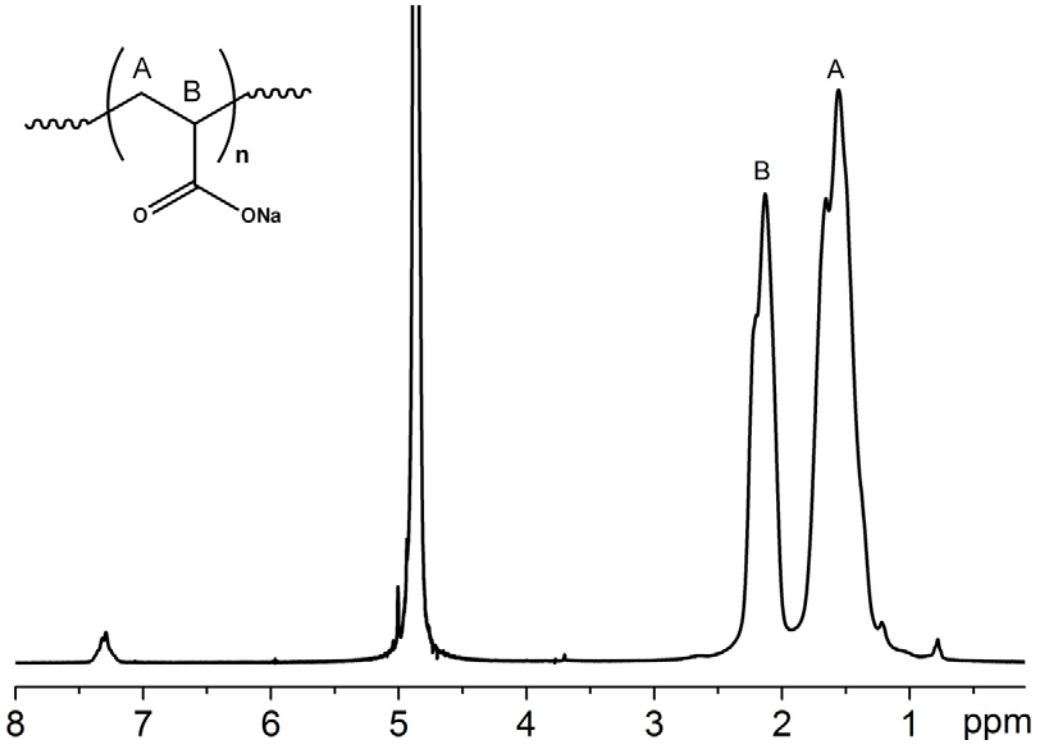

Fig S-1 ^{1}H NMR spectrum of linear PAA

Table S-1 Assignment of observed ^{1}H NMR chemical shifts for linear PNaA (Fig. S-1)

Signal	δ (ppm) observed	δ (ppm), literature[3]	Assignment
A	0.8-1.7	1.3-1.8	-CH_2- (main chain)
B	2.1	1.9-2.3	-CH- (main chain)

Table S-2 Assignment of observed ^{13}C NMR chemical shifts for linear PNaA (Fig. 2a)

Signal	δ (ppm) observed	δ (ppm), literature[4]	δ (ppm), literature[1]	δ (ppm), literature[3]	Assignment
A	36-39	35-38	36	35-39	-CH_2- (main chain)
B	45-47	44-48	39	45-47	-CH- (main chain)
C	185	-	-	185	-COONa (main chain)

The ^{1}H NMR spectrum of the 3-arm star PAA is shown on Figure S-2. The ^{1}H and ^{13}C NMR chemical shift assignments of the 3-arm star PAA are listed in Table S-3 and S-4, respectively. Letters refer to the molecular structures shown on Figure 1.

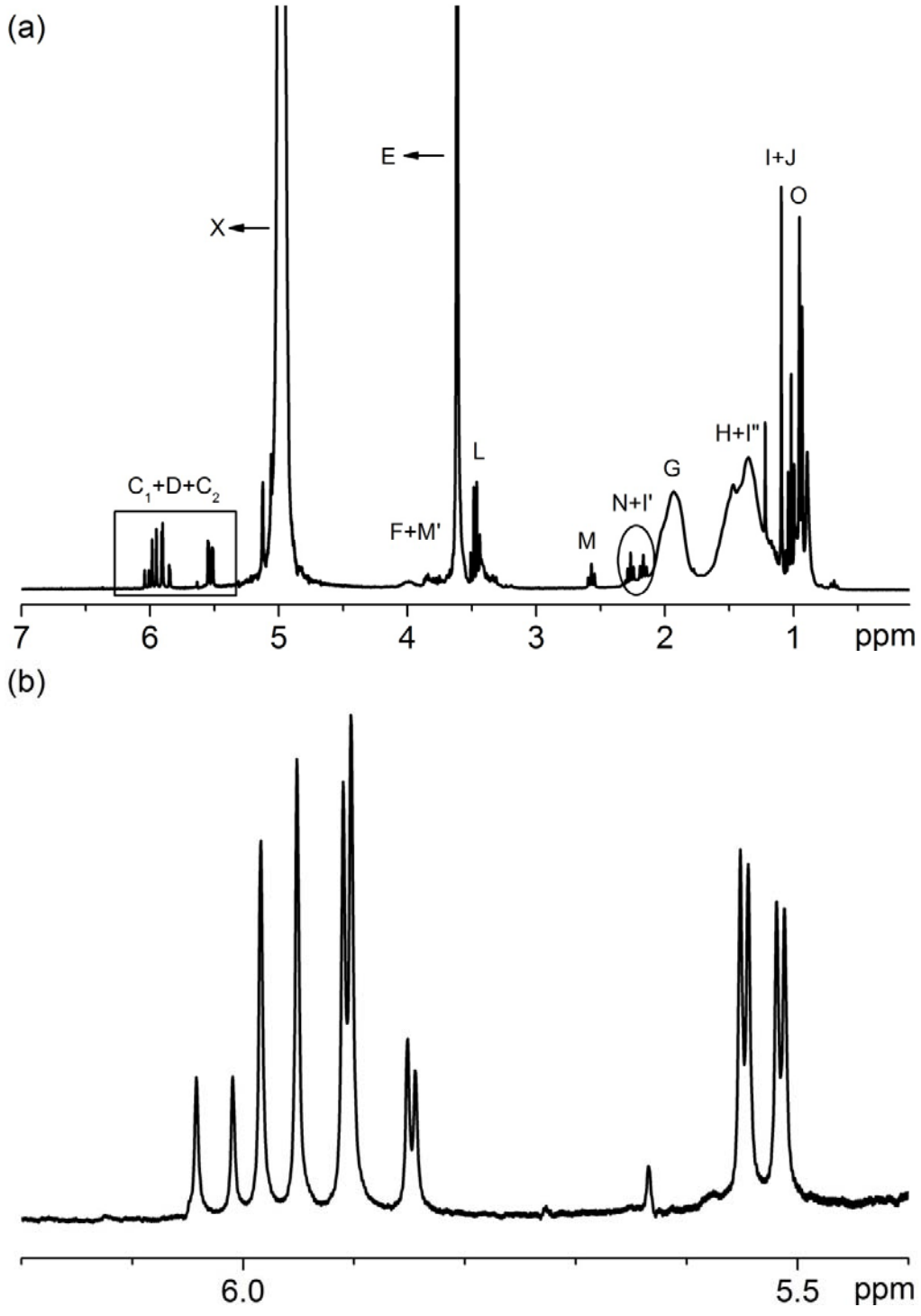

Fig S-2 ^{1}H NMR spectrum of 3-arm star PNaA in D_2O with NaOH: (a) full spectrum, (b) zoom into the residual double bond region showing the splitting pattern

Table S-3 Assignment of observed ^{1}H NMR chemical shifts for 3-arm star PNaA in D_2O with NaOH (Fig. S-2). *The chemical shifts shown in this column were estimated with ChemNMR

Signal	δ (ppm)	δ (ppm) Litera-ture[5]	δ (ppm) Litera-ture [6]	δ (ppm) Estim-ated*	Assignment
C_1	6.7	-	6.53	-	unreacted sodium acrylate monomer, CH_2=CH-COONa, *cis* to COONa
D	5.9-6.0	-	6.15	-	unreacted sodium acrylate monomer, CH_2=CH-COONa
C_2	5-8-5.9	-	5.95	-	unreacted sodium acrylate monomer, CH_2=CH-COONa, *trans* to COONa
X	5.0	4.79	-	-	HOD
F M’	3.5-3.6	-	-	4.1	3-arm star , OH-CH_2-CH_2-CH_2-COR, unreacted alkoxtriacrylate initiator, NaOOC-CH(CH_2)-ONR_2
E	3.5	3.75	-	-	Dioxane
L	3.3-3.4	-	-	3.5	unreacted active site, alkoxtriacrylate, COOCH_2-C_q
M	2.6-2.6	-	-	2.6	SG1, R_1P-CH-NOR_2
N	2.1-2.3	-	-	2.0	-CH_2-CH-COONa
I’		-	-	2.3	3-arm star, CH_2-CH-COONa
G	1.93	-	-	2.4	-CH- (main chain)
H		-	-	1.8	-CH_2- (main chain)
I”	1.4-1.5	-	-	1.9	3-arm star or unreacted alkoxtriacrylate initiator, HO-CH_2-CH_2-CH_2-OR
I					SG1 end group, $(CH_3)_3$-C-NOR
J	1.2	-	-	1.3	SG1 end group, CH_2-CH_3
K					-CH_2-C$(CH_3)_2$-COONa
O	0.9-1.1	-	-	0.9	SG1 end group, $(CH_3)_3$-C-CH-NOR

Table S-4 Assignment of observed ^{13}C NMR chemical shifts for 3-arm star PNaA in D_2O with NaOH (Fig. 2b)**.** *The chemical shifts shown in this column were estimated with ChemNMR

Signal	δ (ppm), observed	δ (ppm) Literature [1]	δ (ppm) Literature [7]	δ (ppm) Literature [3]	δ (ppm) Literature [4]	δ (ppm) Literature [5]	δ (ppm) Literature [6]	δ (ppm) Estim-ated*	Assignment
A	185	-	-	-	-	-	172	173	monomer unit, COONa,
A'	-	-	-	-	-	-	-	185	C_q-COONa,
B		-	-	-	-	-	-	176 (reacted)	3-arm star or unreacted alkoxtriacrylate initiator, COONa
	170	-	-	-	-	-	-	171 (unreacted)	
B'		-	-	-	-	-	172		sodium acrylate, H_3C=CH-COONa
C	135	-	-	-	-	-	133	-	unreacted sodium acrylate monomer, CH_2=CH-COONa
D	127	-	-	-	-	-	128	-	unreacted sodium acrylate monomer, CH_2=CH-COONa
E	67	-	-	-	-	67	-	-	Dioxane
E'		-	-	-	-	-	-	70	SG_1 end group, N-$C(CH_3)_3$
F, L	58-63	-	-	-	-	-	-	62, 59	HO-CH_2-CH_2-CH_2-COR, HO-CH_2-CH_2-CH_2-COR
C_q	50.4	47.4	-	-	-	-	-	-	NaOOC-C_q
G	45-46	39	-	45-47	44-48	-	-	42	-CH- (main chain)
G'		-	-	-	-	-	-		$CONR_1$-$C(CH_3)_2$-CH_2
H	37-39	36	-	35-39	35-38	-	-	-	-CH_2-, main chain
I		-	28	-	-	-	-	-	SG1 end group, -NOC-CH_3
I'		-	-	-	-	-	-	32	CH_2-CH-COONa
I"	28-30	-	-	-	-	-	-	31	3-arm star or unreacted alkoxtriacrylate initiator, HO-CH_2-CH_2-CH_2-OR
J	18	-	17	-	-	-	-	16	SG1 end group, CH_2-CH_3
J'		-	-	-	-	-	-	15	SG1 end group, RON-CH-$C(CH_3)_3$
M	Not detected	-	-	-	-	-	-	81	SG1, R_1P-CH-NOR_2
M'		-	-	-	-	-	-		unreacted alkoxtriacrylate initiator, NaOOC-CH(CH_2)-ONR_2
N	Not detected	-	-	-	-	-	-	50	-CH_2-CH-COONa
K	Not detected	-	-	-	-	-	-	25	CH_2-$C(CH_3)_2$-COONa

The ^{1}H NMR spectrum of the hyperbranched PAA is shown on Figure S-3. The ^{1}H and ^{13}C NMR chemical shift assignments of the 3-arm star PAA are listed in Table S-5 and S-6, respectively. Letters refer to the molecular structures shown on Figure 1.

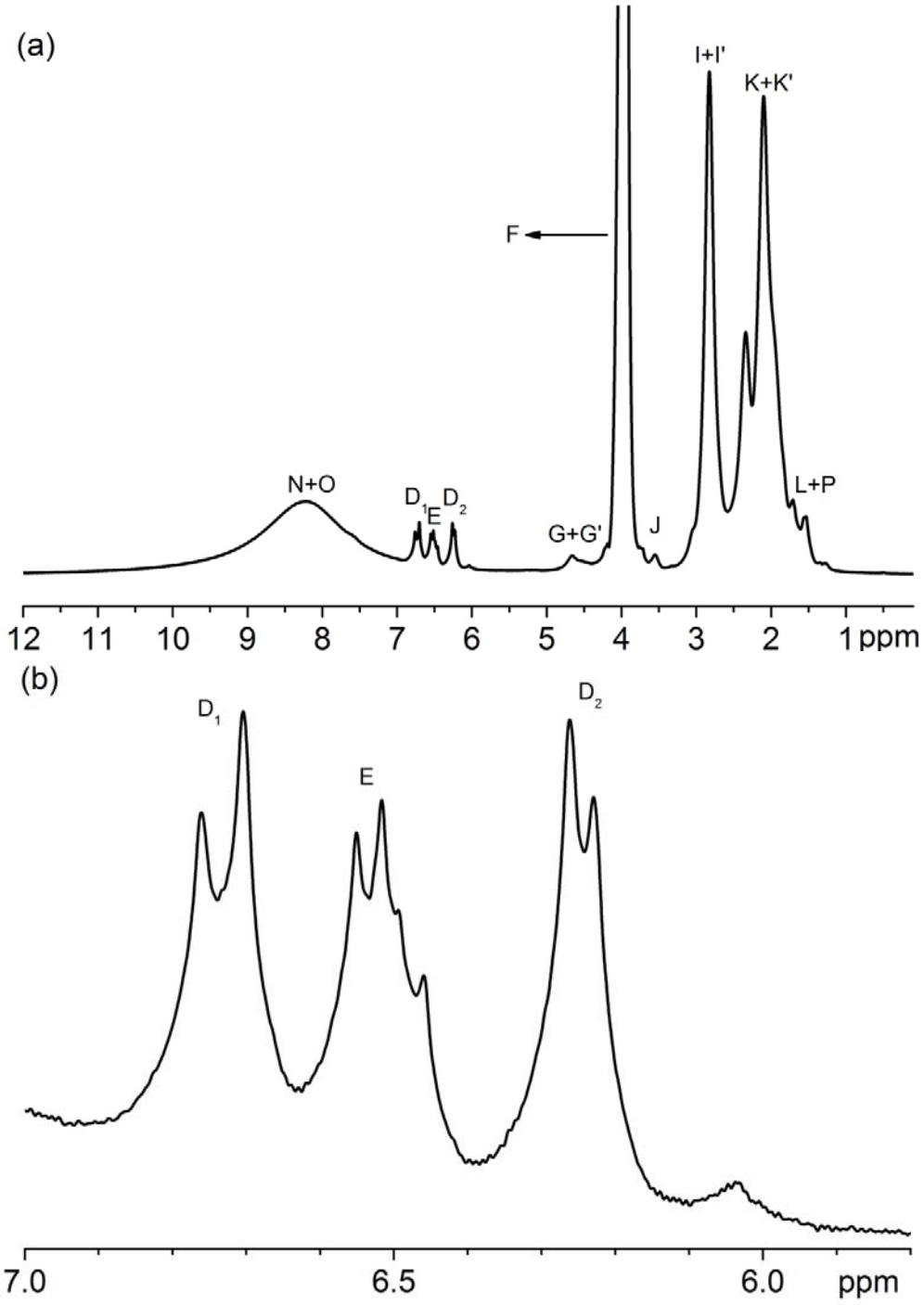

Fig. S-3 ^{1}H NMR spectrum of hyperbranched PAA in 1,4-dioxane-d_8: (a) full spectrum, (b) zoom into the residual double bond region showing the splitting pattern

Table S-5 Assignment of observed ^{1}H NMR chemical shifts for the hyperbranched PAA in 1,4-dioxane-d_8 (Fig. S-3). *The chemical shifts shown in this column were estimated with ChemNMR

Signal	δ (ppm), observed	δ (ppm) Literature [3]	δ (ppm) Literature [5]	δ (ppm) Estimated *	Assignment
N	8.2	-	-	11	-COOH
O		-	-	8.0	R-CONH-R_2
D_1	6.7	-	-	6.3	Inimer with unreacted vinyl group, CH_2=CH-COOR, *trans* to COOR
E	6.5-6.6	-	-	6.1	Inimer with unreacted vinyl group, CH_2=CH-COOR
D_2	6.2-6.3	-	-	5.6	Inimer with unreacted vinyl group, CH_2=CH-COOR, *cis* to COOR
G	4.7	-	-	4.3	Reacted inimer, CH_2-CH_2-COOR
G’				4.6	Unreacted inimer, CH_2-CH_2-COOR
F	3.8-3.9	-	3.75	-	Dioxane
J	3.6	-	-	3.3	(Un)reacted inimer, R_1N-CH_2-CH_2
I, I’	2.8	1.9-2.3	-	-	-CH- (main chain)
K, K’	2.1-2.3	1.3-1.8	-	-	-CH_2- (main chain)
L	1.5-1.7	-	-	1.3	SG1, -RCON-C(CH_3)$_2$
P		-	-		SG1, RP-O-CH_2-CH_3
M	Not detected			0.9	SG1,-CH-C-(CH_3)$_3$

Table S-6 Assignment of observed ^{13}C NMR chemical shifts for the hyperbranched PAA in 1,4-dioxane-d_8 (Fig. 2c). *The chemical shifts shown in this column were estimated with ChemNMR

Signal	δ (ppm), observed	δ (ppm) Literature [5]	δ (ppm) Literature [1]	δ (ppm) Literature [4]	δ (ppm) Literature [3]	δ (ppm) Estimated*	Assignment
A	178	-	-	-	-	178	R_1-CONR$_2$
A'	177					183	main chain, COOH
B	175					174 (reacted)	Inimer with reacted vinyl group, CH_2-CH-COOR
C	167	-	-	-	-	167 (unreacted)	Inimer with unreacted vinyl group, CH_2=CH-COOR, R_1-COO-NHC(=O)-R_2
D	131	-	-	-	-	131	Inimer with unreacted vinyl group, CH_2=CH-COOR
E	129	-	-	-	-	128	Inimer with unreacted vinyl group, CH_2=CH-COOR
F	67	67.19	-	-	-	-	Dioxane
F'	67	-	-	-	-	70	SG1, -RCON-C$(CH_3)_2$
G	64	-	-	-	-	64	Reacted inimer, CH_2-CH_2-COOR
G'	64	-	-	-	-	67	Unreacted inimer, CH_2-CH_2-COOR
G"	64	-	-	-	-	62	SG1, RP-O-CH_2-CH_3
H	48	-	47.4	-	-	-	COOH-C_q
I, I'	42	-	39	44-48	45-47	-	-CH- (main chain)
J	40	-	-	-	-	39	(Un)reacted inimer, R_1N-CH_2-CH_2
J'						39	Unreacted inimer, CONR$_1$-C$(CH_3)_2$-CH_2
K, K'	36	-	36	35-38	35-39	-	-CH_2- (main chain)
K"						35	Reacted inimer, CONR$_1$-C$(CH_3)_2$-CH_2
L	32	-	-	-	-	26	SG1, -RCON-C$(CH_3)_2$
L'		-	-	-	-	26	(Un)reacted inimer, -C$(CH_3)_2$
M		-	-	-	-	27	SG1,-CH-C-$(CH_3)_3$
Q	Not detected					81	SG1, R_1P-CH-NOR$_2$
P	Not detected					16	SG1, RP-O-CH_2-CH_3
R	Not detected					15	SG1, NOR$_1$-CH-C-$(CH_3)_3$

Capillary electrophoresis

The separations presented in this work are counter-electroosmotic flow (see Fig. S-4).

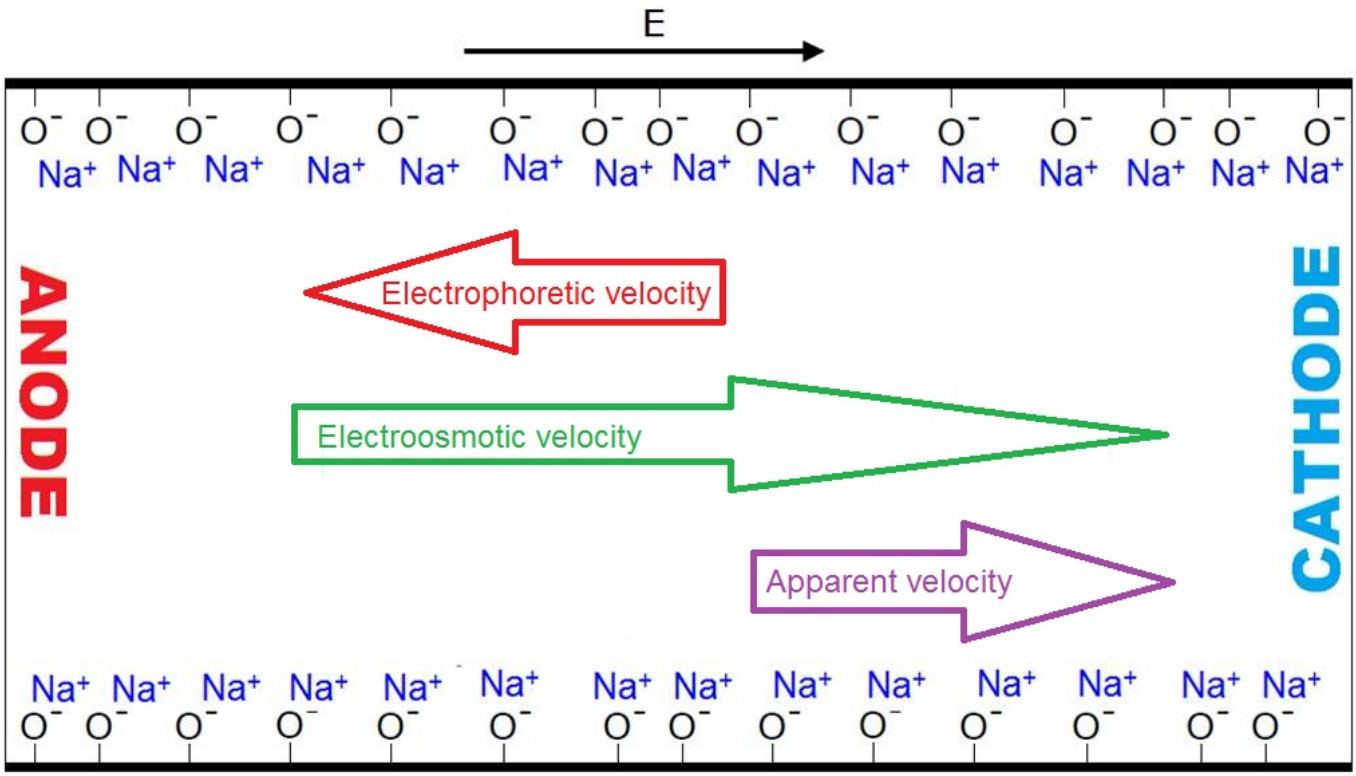

Fig. S-4 Fused-silica capillary filled with buffer with vectors representing the electroosmotic flow (EOF) and the electrophoretic mobility in which the electrophoretic velocity combined with the electroosmotic velocity results in the apparent velocity

The migration time depends on the electrophoretic mobility and the EOF. The EOF is influenced by numerous factors which can result in variations in migration time. For this reason, the electrophoretic mobility is a reproducible quantity and is shown in this manuscript rather than migration time for the separation of PAA salts. More importantly, the electrophoretic mobility, m_{ep}, represents the intrinsic velocity of the PAA salts along the capillary whilst also correcting for the EOF:[8]

$$m_{ep} = \frac{l.L}{V}\left(\frac{1}{t_M} - \frac{1}{t_{eo}}\right) \quad \text{(S-1)}$$

where l is the distance from the capillary inlet to the capillary detection window in cm (0.535 m), L is the total capillary length (0.620 m), V is the electric field applied to the capillary (30,000 V), t_M and t_{eo} are the migration times of the PAA samples and of the neutral species, respectively. The unit of the electrophoretic mobility is $m^2.V^{-1}.s^{-1}$.

The Poiseuille equation was used to determine the injection volume (V_t):

$$V_t = \frac{\Delta P D^4 \pi}{128 \eta L} \quad \text{(S-2)}$$

where, D is the internal diameter of the capillary, η is the viscosity, L is the total length of the capillary, and ΔP is the difference in the change of pressure in the capillary, taken respectively as 50 μm, 10^{-3} Pa.S (1 cP), 0.62 m and 30 mbar .

Table S-7 Electrophoretic mobilities m_{ep} (10^{-8} $m^2 \cdot V^{-1} \cdot s^{-1}$) of linear, 3-arm star and hyperbranched PNaA as well as their relative standard deviations (RSD). PNaA samples were prepared and injected under the conditions stated in the Materials and Methods section unless specified otherwise. Some PNaA samples were injected with half the concentration of the sample (blue) or half the injection time (red). The hyperbranched PNaAs were dissolved in three different ways: dissolved in 1.5 mL water (green) or with an additional 15 µL of 1 M NaOH (black) or 30 µL of 0.5 M $Na_2B_4O_7.10H_2O$ (orange). A and B are the two different operators.

	Linear PNaA			**3-arm star PNaA**			**Hyperbranched PNaA**		
	Date	$m_{ep,A}$	$m_{ep,B}$	**Date**	$m_{ep,A}$	$m_{ep,B}$	**Date**	$m_{ep,A}$	$m_{ep,B}$
	01/03	3.60		05/03	3.52		05/03	3.50	
	01/03	3.61		05/03	3.52		05/03	3.50	
	05/03	3.58		28/05	3.49		13/03	3.59	
	05/03	3.54		24/07		3.54	13/03	3.59	
	13/03	3.58		24/07		3.55	13/03	3.52	
	13/03	3.54		25/07		3.58	13/03	3.52	
	11/04	3.75		25/07		3.59	28/05	3.45	
	11/04	3.75		27/07		3.58	24/07		3.48
	28/05	3.51		27/07		3.58	24/07		3.48
	24/07		3.54	27/07		3.58	25/07		3.51
	24/07		3.55	27/07		3.59	25/07		3.52
	25/07		3.56	07/08		3.49	27/07		3.53
	25/07		3.57	07/08		3.50	27/07		3.53
	27/07		3.57	07/08		3.47	07/08		3.45
	27/07		3.59	07/08		3.47	07/08		3.46
	27/07		3.62	07/08		3.47	07/08		3.47
	27/07		3.63	07/08		3.48	07/08		3.47
	07/08		3.55				07/08		3.49
	07/08		3.56				07/08		3.50
	07/08		3.57						
	07/08		3.59						
	07/08		3.57						
	07/08		3.60						
Average		3.61	3.58		3.51	3.53		3.53	3.49
Overall Average		3.59			3.53			3.50	
SD		0.09	0.03		n/a	0.05		0.05	0.03
Overall SD		0.06			0.05			0.04	
RSD %		2.41	0.76		n/a	1.46		1.45	0.79
Overall RSD%		1.63			1.34			1.15	

The separations presented in Figure 5 in sodium borate were reproduced in ammonium acetate (Fig. S-5). It is to be noted that ammonium acetate injections have a significantly lower throughput than the borate one (technical issues requiring reinjection, such as current leak, were common with ammonium acetate while barely occurring with borate buffer).

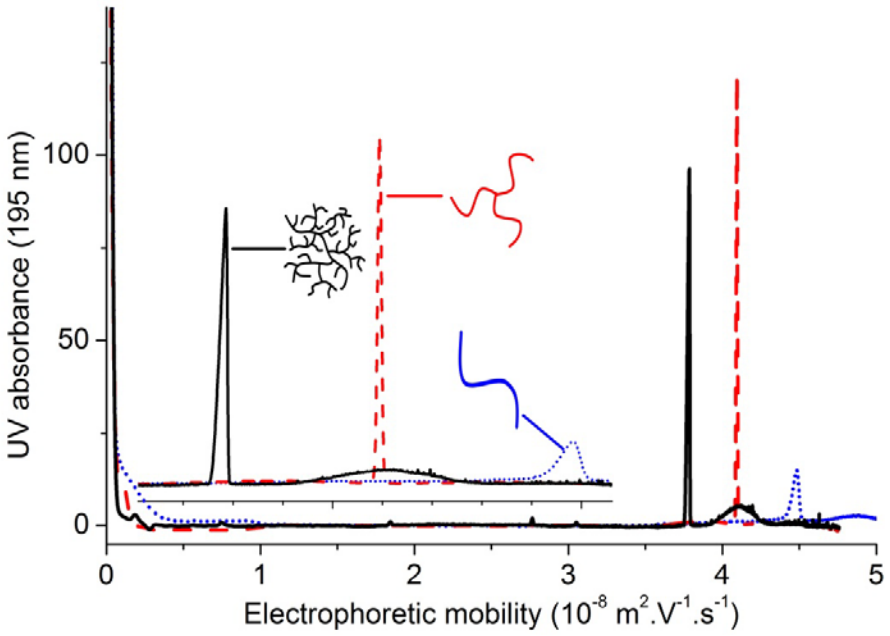

Fig. S-5 Separation of PNaA according to their branching topologies: linear (blue dotted line), 3-arm star (red dashed line) and hyperbranched (black solid line) PNaA in AA75

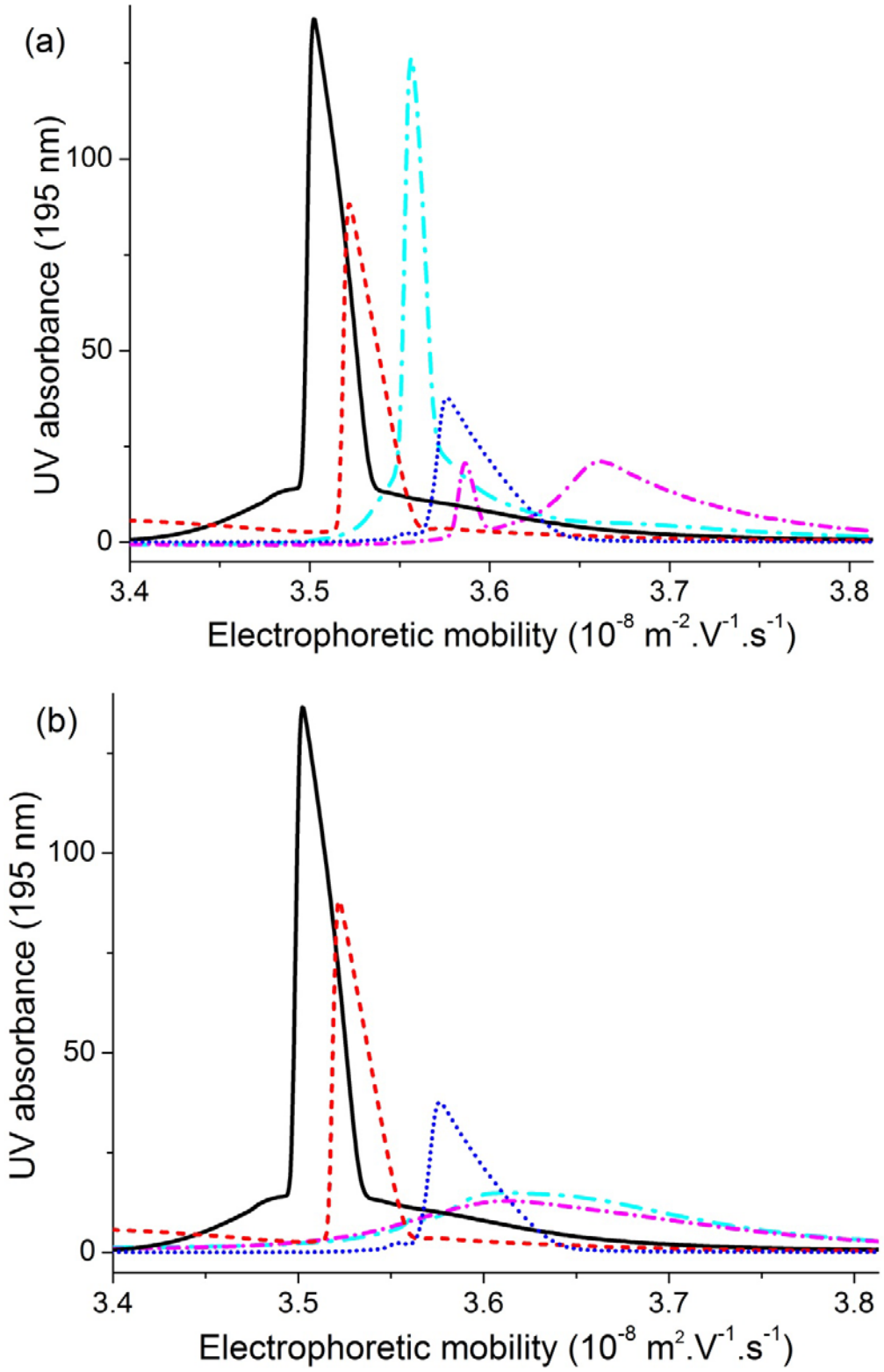

Fig. S-6 Electropherogram of a) NMP-PAA1 (light blue dashed-dotted line) and NMP-PAA2 (purple dashed-dotted line), as well as of b) NMP-PtBA1 (light blue dashed-dotted line) and NMP-PtBA2 (purple dashed-dotted line). In both cases, the hyperbranched (black solid line), 3-arm star (red dashed line) and the linear (blue dotted line) PNaA are shown as well

In their mass spectrometry analysis, Barrere et al. degrade selectively the *tert*-butyl part of the SG1 end-groups of poly(ethylene oxide) (PEO), polystyrene (PS) and poly(n-butyl acrylate) (PnBA).[9] They use 10.01 $mg \cdot mL^{-1}$ of silver trifluoroacetate, corresponding to $3.93.10^{-5}$ $mol \cdot L^{-1}$ of trifluoroacetate (TFA). The ratio TFA to SG1 end-groups used in [9] and in our work are compared in Table S-8.

Table S-8 Comparison of conditions used to degrade polymer SG1 end-groups in [9] and in this work.

Taken from [9]			**Calculated from [9]**		**This work**			**Comparison**
Polymer	**Polymer concentration (mg/mL)**	**M_n polymer**	**Polymer chains concentration (10^3 mol/L)**	**TFA per polymer chains, mol/mol**	**M_n PtBA**	**TFA per *tert*-butyl groups mol/mol**	**TFA per polymer chains, mol/mol**	**TFA in our work to [9]**
PEO	4	2000	2.00	50.9	7500	5	293	5.8
PEO	4	5000	0.80	20.4				14.4
PS	4	2300	1.74	44.2				6.6
PnBA	4	6000	0.67	17.2				17.3

References

1. Couvreur L, Lefay C, Belleney J, Charleux B, Guerret O, Magnet S (2003) First Nitroxide-Mediated Controlled Free-Radical Polymerization of Acrylic Acid. Macromolecules 36:8260-8267
2. Garces FO, Sivadasan K, Somasundaran P, Turro NJ (1994) Interpolymer complexation of poly(acrylic acid) and polyacrylamide: structural and dynamic studies by solution- and solid-state NMR. Macromolecules 27:272-278
3. Ladaviere C, Dorr N, Claverie JP (2001) Controlled radical polymerization of acrylic acid in protic media. Macromolecules 34:5370-5372
4. Loiseau J, Doerr N, Suau JM, Egraz JB, Llauro MF, Ladaviere C (2003) Synthesis and characterization of poly(acrylic acid) produced by RAFT polymerization. Application as a very efficient dispersant of CaCO3, kaolin, and TiO2. Macromolecules 36:3066-3077
5. Gottlieb HE, Kotlyar V, Nudelman A (1997) NMR Chemical Shifts of Common Laboratory Solvents as Trace Impurities. J. Org. Chem. 62:7512-7515
6. Spectral database for organic compounds SDBS, http://www.aist.go.jp/RioDB/SDBS/cgi-bin/cre_index.cgi
7. Guillaneuf Y, Couturier J-L, Gigmes D, Marque SRA, Tordo P, Bertin D (2008) Synthesis of Highly Labile SG1-Based Alkoxyamines under Photochemical Conditions. J. Org. Chem. 73:4728-4731
8. Castignolles P, Gaborieau M, Hilder EF, Sprong E, Ferguson CJ, Gilbert RG (2006) High-resolution separation of oligo(acrylic acid) by capillary zone electrophoresis. Macromol. Rapid Commun. 27:42-46
9. Barrere C, Chendo C, Phan TNT, Monnier V, Trimaille T, Humbel S, Viel S, Gigmes D, Charles L (2012) Successful MALDI-MS Analysis of Synthetic Polymers with Labile End-Groups: The Case of Nitroxide-Mediated Polymerization Using the MAMA-SG1 Alkoxyamine. Chem. Eur. J. 18:7916-7924